東 海 大 學 資 訊 工 程 學 系 研 究 所

碩士論文

指導教授：呂芳懌 博士

Dr. Fang-Yie Leu

以智慧型手機判斷跌倒及分類日常動作

Fall Detection and Motion Classification by Using Mobile Phone

研究生： 林怡岑

Author: Yi-Chen, Lin

中華民國 一〇五 年 七 月

July, 2016

東海大學碩士學位論文考試審定書

東海大學資訊工程學系 研究所

研究生 林 怡 岑 所提之論文

以智慧型手機判斷跌倒及分類日常動作

經本委員會審查，符合碩士學位論文標準。

學位考試委員會

召 集 人 陳金鈴 簽章

委 員 [illegible]

余心淳

蔡坤霖

指 導 教 授 [illegible] 簽章

中華民國 105 年 7 月 20 日

致謝

非常感謝呂芳懌教授從大學專題到研究所以來悉心的指導與提攜，研究進行期間更指引論文方向。也非常感謝柯佳吟教授，多次給予論文相關的指教與討論。感謝父母給我的支持，讓我能在沒有經濟壓力的環境下安心的進行我的研究，更在我遭遇瓶頸的時候給我的鼓勵及建議。感謝林修翰學長及資料庫實驗室莊勝傑、陳信良及劉晉宇學長，在論文撰寫期間給予的幫助。最後，感謝鄭至超先生給我很多實際應用及發展的建議和在英文撰寫上的幫助。

TUNGHAI UNIVERSITY COMPUTER SCIENCE DEPARTMENT
1981
東海大學
資訊工程學系

摘要

跌倒是中老年人受傷的常見原因。每三位老人就有一人曾發生跌倒，一旦發生跌倒，有兩倍的機率會再次跌倒，五分之一的跌倒會導致嚴重的傷害。最常見因跌倒而住院治療的傷害是頭部傷害和髖部骨折。髖部骨折通常都是側身跌倒引起的。自動偵測跌倒時的姿勢可以在跌倒事件突然發生時，快速地判斷出可能發生的傷害。此外，知道跌倒發生的原因及方式不僅有助於再次跌倒之預防及管理，更可以快速的做出有針對性的應急反應。在本篇論文中，我們使用三軸加速度計及陀螺儀偵測日常生活上之動作與判斷是否跌倒。我們先分析跌倒時各種動作與跌倒所產生之訊號之間的關係及所代表的意義。再將跌倒細分成六大項：向前撲倒、向後滑倒、向左及向右跌倒、向後跌倒時向左及向後跌倒時向右轉身。最後，使用決策樹從所產生之信號來判斷日常生活動作及跌倒類型。經實驗結果，研判跌倒的準確率達 98.46%，加上分辨跌倒的動作後的準確率為 95.38%。

東海大學
資訊工程學系

關鍵詞：

資料探勘、決策樹、智慧手機、三軸加速器、陀螺儀、跌倒動作判斷、日常動作判斷

Abstract

Falls are a common cause of injury for the elderly all over the world. One out of three elderlies is injured from falling each year. Research indicates that once they fall, the probability of them falling again doubles, and one out of five elderly falls often cause a serious injury. Most are the head injury and hip fracture. The reason of causing hip fracture is falling sideways. In fact, falls of an elderly cannot be anticipated and falls are hard to detect. In addition, people carry their mobile phones almost all the time. Therefore, in this study, a mobile application for fall management, named the Fall Detection System using Mobile Phone (FDSMP) is developed to detect falls automatically. With a mobile phone, an elderly fall can be detected immediately almost when the fall occurs. The reaction time, defined as the time period between the occurrence of the fall event and the time when caregivers arrive at the place where the elderly falls can be then shortened, meaning the required first aid can be remedy quicker and more accurately. The application will also tell us what type of fall has occurred. In this study, two *microelectromechanical systems* (MEMSs), i.e., Triaxial accelerometer and gyroscope installed in a mobile, are employed to detect falls and a person's daily movements. Then the correlation between the actions of a falling (or a movement) and the signals collected by the two MEMSs are analyzed so as to differentiate whether the person is doing an *activity of daily living* (ADL) or the user falls. We subdivided fallings into six types: Falling forward, Falling backward, Falling right, Falling left, Body

turning right while falling backward, Body turning left while falling backward. The differentiation and subdivision are performed by using a decision tree. Our experimental results showed that the accuracy of fall detection and ADL classification is 98.46% and that of the falling classification is 96.57%.

TUNGHAI UNIVERSITY COMPUTER SCIENCE DEPARTMENT
1981
東海大學
資訊工程學系

Keywords:

Data mining, Decision Tree, Mobile Phone, Gyroscope, Triaxial Accelerometer, Fall, Motion Classification

Table of Contents

東海大學 資訊工程學系

List of Figures

TUNGHAI UNIVERSITY COMPUTER SCIENCE DEPARTMENT
1981
東海大學
資訊工程學系

List of Tables

TUNGHAI UNIVERSITY COMPUTER SCIENCE DEPARTMENT
1981
東海大學
資訊工程學系

1. Introduction

In recent decades, aging population is a popular phenomenon in many countries. Between 2015 and 2030, the number of people in the world aged 60 years or over is projected to grow by 56 percent, from 901 million to 1.4 billion, and by 2050, the global population of older persons will be more than double the size in 2015, reaching nearly 2.1 billion [1]. With the increase of age, an elderly will gradually lose user's ability of self-care. How to properly take care of the elderly has been a hot research topic nowadays. To successfully do this, we must look into its unavoidable problems. Elderlies above the age of 65 risks a one-third chance of falling each year [2][3]. Research indicates that the risk of falls increases proportionally with aging. But only less than one-half of the cases were reported to their doctors [2]. Once a fall occurs, the chance of fall again doubles in the coming one year. In fact, one-fifth of falls causes serious injury, including hip fractures and traumatic brain injuries. Such injuries are the main cause of hospitalization of elderlies. Hip fractures very often are resulted from falling sideways [3].

The consequences of falls tend to be huge, especially for older people, very usually causing reduced quality of life, serious injuries, increased risk of death, increased fear of falling and restriction of activities [4]. The injuries are not only physical but also psychological. Ironically, the fear of falling make an elderly to have a higher risk of falling. Previous studies have shown that their proposed systems only determine whether a fall occurs, e.g., Albert [5] only discriminated four kinds of falls. In fact, falls are complex events. In addition, the use of machine learning can enhance the system ability to analyze falls and classify activity of daily living (ADL). Therefore, in this chapter, we develop a fall management system, named Fall Detection System using Mobile Phones (FDSMP), which utilizes the microelectromechanical systems (MEMSs)

installed in a mobile phone, including a Triaxial accelerometer and a gyroscope, and decision tree techniques to detect and classify falls and ADLs. Once a fall occurs, through the instant messaging communications and the convenience of the FDSMP, caregivers can know the event immediately and provide required assistance when necessary.

Our experimental results show that the FDSMP demonstrates a success of body M-class, which in turn enhances the accuracy for determining fallings, and correctly identifies the fall types, such as Falling forward, Falling backward, Falling right, Falling left, Body turning right while falling backward and Body turning left while falling backward. The accuracy of all types of detections is 98.46% and that of fall classification is 96.57%.

The result of this chapter is organized as follows. Section 2 introduces related studies of this chapter. Section 3 describes the materials and methods used in tis study. Section4 shows our implementation. Evaluation presented in Section5. Sections 6 and 7 respectively concludes this chapter and lists our future work and challenges.

東海大學
資訊工程學系

2. Related Work

A lot of fall-detection approaches have been studied [6][7][8][9][10][11][12]. Bai *et al.* [6] used an Accelerometer and a GPS installed in a smart phone to design a fall monitor and position identification system. They analyzed the change of acceleration and six typical actions of human beings. The latter includes going upstairs, going downstairs, standing up, sitting down, running and jumping. He *et al. [7]*, utilized calculated signal magnitude area (SMA), signal magnitude vector (SMV) and tilt angle (TA) to determine the threshold for a fall. They presented a system which classified human motions in real-time with a smartphone mounted on the user's waist. A built-in Triaxial accelerometer collects data of body motions, with which the smartphone is also able to classify the motions into five different patterns: vertical activity, lying, sitting (or static standing), horizontal activity and fall.

Zhang *et al.* [8] employed a Triaxial accelerometer equipped in a cellphone to collect SMV values, and utilized 1-Class Support-Vector Machine algorithm for preprocessing and Kernel Fisher Discriminant, and k-NN (K-Nearest Neighbor) algorithm for precise classification. They found that this method can detect falls effectively and make less disturbance to people's daily living than the general wearable sensors do. Bourke *et al.* [9] used simulated falls performed under supervised conditions, and ADLs done by elderly subjects. The ability to discriminate between falls and ADLs relies on Triaxial accelerometer sensors mounted on the trunk and thigh. Data was analyzed using the MATLAB to determine the peak accelerations recorded for eight different types of falls, including forward falls, backward falls, lateral falls left and lateral falls right (four movements), performed on two conditions, i.e., legs straight and flexed. Falls detection algorithms were devised using threshold techniques.

Sposa *et al.* [10] presented an alert system which used common commercially available electronic devices to detect falls, and alerted authorities on an Android-based smart phone with an integrated Triaxial accelerometer. Data from the accelerometer is evaluated with several thresholds-based algorithms and position data to determine a fall. The threshold is adaptive based on parameters, such as height, weight, and level of activity, provided by users.

Some researchers added other auxiliary sensors to their detectors. Hwang *et al.* [11] designed an algorithm for the detection of falls using smartphones equipped with Triaxial accelerometer and magnetometers. They also proposed a fall detection method that recognizes a fall if the magnitudes of an acceleration and angular displacement exceed given thresholds. Experiments for detecting falls are performed in four directions: fall forward, fall backward, fall left, and fall right. Data is collected from 200 experimental falls, in each of which a smartphone is fastened on a belt worn around the waist. An overall detection rate is 95%, and those of fall forward, backward falls, leftward falls and rightward falls are 94%, 100%, 94% and 92%, respectively.

In [12] by Doukas *et al.*, sensors equipped with accelerometers and microphones are attached to the body of the patients, and transmit patient's movement and sound data wirelessly to the monitoring unit. The sound and movement are classified by using Support Vector Machines. Rakhman *et al.* [13] and Dai *et al.* [14] added a gyroscope as an assistance device. Dai *et al.* [14] first designed a fall detection algorithm based on mobile phone platforms and proposed PerFallD, which is a pervasive fall detection system implemented on mobile phones. Noury *et al.* [15] proposed 20 scenarios and 10 fall types to evaluate fall sensors. Li *et al.* [16] classified falls into 6 types and 12 kinds of ADLs. Other state-of-the-art fall detection systems can be found in [17][18][19] .

Zhao *et al.* [20] divided human movements into four types, including stationary, walking, running and fall, and analyzed relevant data with a Decision tree. The results show that the precision is 100% and the recall is 75.8%. Aguiar *et al.* [21] discussed the accuracies for Decision tree, K-nearest neighbors (K-NN) and Naïve Bayes and claimed that Decision tree outperforms the others. The sensitivity of the case in which mobile phones is placed in pockets is 94% and on belts is 90.6%. The specificity in pockets is 90.2% and on belts is 96.1%, and the accuracy in pocket is 92% and on belts is 93.7%. In the classification systems presented by Zhao *et al.* in [20] and Aguiar *et al.* in [21], the precision is 86%, and recall is 100%. After adding a gyroscope as an auxiliary device, the precision is 97.4%, and recall is 100%. That means a gyroscope is helpful in classification.

Albert *et al.* [5] found that there was a ceiling phenomenon, which is the case when acceleration of gravity is greater than a specific value, no higher value can be measured and shown due to the limitation of the maximum (minimum) acceleration that a Triaxial accelerometer can detect. He *et al.* [7] using the Lenovo Le-Phone in 2012, Beauvais *et al.* [22] utilizing the Samsung Galaxy SII in 2014 and Aguia *et al.* [21] employing in 2012 all have the same situation. In fact, when we conduct experiments with the mobile phones produced earlier than 2015, the values obtained are not quite accurate. It is recommended to use the smartphones manufactured in 2015 or after, and suitability of chip used needs to be ascertained.

As most people like to use mobile phones, the sizes of which are bigger than four inches, it is hard to place them on the waist or leg, particularly prone to cause serious damage to the phone at the time of running, jumping or sitting down. Fang *et al.* [23] showed that when the mobile phones are placed on the chest, waist and thigh, the sensitivities were 72.22%, 56.67% and 53.33%, respectively, and specificities were

73.78%, 66.39% and 57.22%, respectively. Accuracy of placing the mobile phones on the chest is apparent higher than those of others. Therefore, in this study, during experiments, the used mobile phone is placed in testers' chests.

TUNGHAI UNIVERSITY COMPUTER SCIENCE DEPARTMENT
1981
東海大學
資訊工程學系

3. Materials and Methods

3.1 Research methods

At present, studies that utilize mobile phones to detect falls mainly rely on Triaxial accelerometer. However, like the cases in [13] and [14], a gyroscope as an auxiliary micro-electronic device is employed by the FDSMP to detect a user's body rotation angle. A Decision tree is also utilized to classify a movement in a systematic way. The FDSMP further uses an industrial technology which integrates both mechanical engineering and microelectronics technology as a MEMS. An MEMS usually contains a microprocessor and multiple micro-sensors to obtain external information [24]. The size of an MEMS is determined by the sizes of its components, which are often between 1 and 100 microns (0.001 to 0.1mm). The sizes of MEMS devices typically range between 20 microns and one millimeter. With the advancement of sensor techniques, the complexity and efficiency of MEMSs continue to improve. Within a mobile phone, the Triaxial accelerometer and gyroscope sense the phone's Triaxial accelerations and directional changes, respectively. Experiments are conducted with a user standing right behind the mobile phone, i.e., facing the same direction with the phone.

(1) Triaxial Accelerometer

The acceleration detected by a Triaxial accelerometer as shown in Figure 1 is divided into x, y and z three sub-accelerations. The unit of the triaxial accelerometer is g ($9.8\mathrm{m/s^2}$). The direction of triaxial accelerometer is as follows. The left side of the person, who stands behind the mobile phone, is the positive direction of x-axis. The right side, of course, is negative. The upside (down side) of the y-axis is positive

(negative). The forward (backward) of the z-axis is positive (negative).

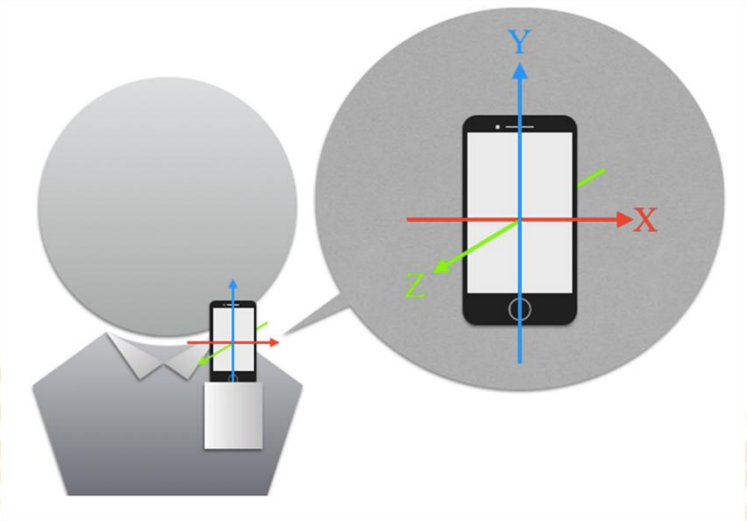

Figure 1.The three axis of a Triaxial accelerometer equipped in a mobile phone

(2) Gyroscope

A gyroscope, as a device designed to measure and maintain a sense of rotational direction based on the theory of conservation of angular [25][26], mainly consists of a rotatable rotor. When the gyroscope starts to rotate, the rotor angular momentum tends to resist the change of direction.

(a) Direction of a rotation (b) Directions of a gyroscope

Figure 2. Pitch, Roll and Yaw of a gyroscope equipped in a mobile phone

Gyroscopes are popularly utilized by navigation and positioning systems. The unit

of the gyroscope is degree (°). The directions of its three axis are shown in Figure 2-b. Pitch is the rotation along the x-axis; the forward is positive. Of course, the backward is negative. Roll is the rotating along the y-axis. Rotating to the left (right) is positive (negative). Yaw is the rotating along the z-axis; rotation to the right (left) is positive (negative).

In our everyday life, many ADLs can be found. However, in this study, we only choose standing up, sitting down, walking and running since they are our most frequent daily activities. Falls according to [15], as listed in the first two columns of Table 1, can be classified into Backward fall ending lying, Backward fall ending in later position…. In this study, as mentioned above, we classify the movements of falls into six types, including Falling forward, Falling backward, Falling right, Falling left, Body turning right while falling backward and Body turning left while falling backward.

1981
東海大學
資訊工程學系

Table 1. The classification in [15] are listed in the first two columns. The third column is the classification of the FDSMP.

<table>
<tr><th colspan="2">Fall direction</th><th>Ending state</th><th>FDSMP</th></tr>
<tr><td colspan="2" rowspan="3">Backward</td><td>lying</td><td rowspan="3">Falling backward</td></tr>
<tr><td>In lateral position</td></tr>
<tr><td>In the knees</td></tr>
<tr><td rowspan="4">Forward</td><td rowspan="2">Directly</td><td>With forward</td><td rowspan="4">Falling forward</td></tr>
<tr><td>Lying flat</td></tr>
<tr><td rowspan="2">With rotation</td><td>In lateral right position</td></tr>
<tr><td>In lateral left position</td></tr>
<tr><td rowspan="2">Lateral</td><td>Right</td><td>Lying flat</td><td>Falling right</td></tr>
<tr><td>Left</td><td>Lying flat</td><td>Falling left</td></tr>
<tr><td colspan="2">-</td><td>-</td><td>Body turning right while falling backward</td></tr>
<tr><td colspan="2">-</td><td>-</td><td>Body turning left while falling backward</td></tr>
</table>

3.2 Signal Processing

After receiving signals from a smart phone, we use SMV and angular variation, denoted by A_t, to calculate the strength and the angle of a fall, where the SMV and A_t are calculated as follows.

$$\text{SMV} = \sqrt{X^2 + Y^2 + Z^2} \tag{1}$$

in which X, Y and Z, respectively, represents the acceleration values of gravity in the Triaxial (i.e., X, Y and Z) directions, where $A_{t-1}$is the last angular variation,

ω is the measured angular velocity by gyroscope.

$$A_t = A_{t-1} + \omega \cdot \Delta t \quad (2)$$

In the signals received, the maximum SMV value of each human action, and maximum and minimum values of the variation of rotation angles are identified. Note that, the Pitch that turns forward, as an example, is positive, the angle changing the most in the forward direction is the maximum, and the angle changing the most in the backward direction is the minimum. The Roll's and Yaw's are similar.

TUNGHAI UNIVERSITY COMPUTER SCIENCE DEPARTMENT
1981
東海大學
資訊工程學系

4. Implementation

4.1 Features of Six Falling Movements

The maximum and minimum of Pitch, Roll and Yaw of the 6 falling movements we choose are shown in Table 2, in which Falling forward (Falling backward) has the maximum (minimum) values of Pitch. Falling right (Falling left) mainly is dominated on the angle of Yaw, so it has a maximum (minimum) value. Body turning right while falling backward and Body turning left while falling backward trigger both the Pitch and then Roll (see Table 2). Since both the two fallings are reclined (falling backward), there is a minimum in the negative direction of Pitch. The body rolling in the right spin (turning right) produces a minimum in the negative direction of Roll. Rotating/truing to the left during falling results in a maximum in the positive direction of Roll.

Table 2. Features of the Six Fallings.

Classify	Falling forward	Falling backward	Falling right	Falling left	Body turning right while falling backward	Body turning left while falling backward
Pitch	Maximum	Minimum	-	-	Minimum	Minimum
Roll	-	-	-	-	Minimum	Maximum
Yaw	-	-	Maximum	Minimum	-	-

4.2 Classifiers

The Weka [27], as a data mining tool, provides different classification mechanisms, called classifiers, including decision tree, Rule-PART, Bayes Theorem, Rule-DTNB, Meta-Bagging, and so on. In this study, we choose some of them to analyze and classify the data collected by using the two utilized MEMSs. Their classification accuracies are listed in Table 3.

Table 3. Classification accuracies of classifiers tested in this study.

Classifier	Tree			Rules		Bayes	Meta		
	J48	NBTree	BFTree	PART	DTNB	BayesNet	Attribute Selected Classifier	Bagging	Filtered Classifier
Accuracy	98.46%	98.46%	96.92%	98.46%	96.92%	98.4615%	98.46%	96.92%	96.92%
TP	1	1	0.973	1	0.973	1	0.973	1	1
FP	0.036	0.036	0	0.036	0.036	0.036	0	0.071	0.036
Precision	0.974	0.974	1	0.974	0.973	0.974	1	0.949	0.974
Recall	1	1	0.973	1	0.973	1	0.973	1	1
F-Measure	0.987	0.987	0.986	0.987	0.973	0.987	0.986	0.974	0.987

4.2.1 Decision Tree

Decision tree is a popular decision support tool often used to decide the outputs for input data (e.g., determining the possible results of random events), the outcomes on given resources, and the cost effectiveness of a constructed structure (e.g., a tree or model). Decision Trees are commonly used in operation research, especially to determine the most that a strategic objective can achieve. The decision

rules of a decision tree can be linearized [28], wherein the result is the content of a leaf node, e.g., node *N*, and decision making is the process determining the path that will finally reach *N* as the final result based on the values of input parameters. In fact, the path can be expressed as rules with the format: **if** $AND_{i=1}^{n}\ Condition\ i$, **then** *Result*, meaning there are *n* conditions, $n \geq 1$, i.e., there are *n* links from the root to *N*, and *Result* is the content of the leaf node. In other words, the path has *n*+1 nodes.

J48 is an open source of the C4.5 decision tree algorithm implemented with Java [29] by Quinlan [30]. This algorithm can be used to classify input data. So it is often called statistical classifier [31], and it is a remarkable mining algorithm Ranked # 1 announced by the Springer LNCS [32].

4.2.2 Rule - PART

PART, as a scheme used to generate accurate rule sets for a decision tree, is proposed by Eibe and Witten [33]. The PART has two dominant schemes for rule-learning, i.e., C4.5 and RIPPER, and shows how good rule sets can be learned without any need for global optimization. They present an algorithm for inferring rules by repeatedly generating partial decision trees, consequently combining the two major paradigms, i.e., creating rules from decision trees and the separate-and-conquer rule-learning technique, for rule generation.

4.2.3 Bayes Theorem

Bayes' Theorem is developed based on a probability theory. There is a random variable with the probability of the conditions and the edge probability distribution. The conditioned probability of random events A and B is defined as follows [34].

$$P(A|B) = \frac{P(B|A)P(A)}{P(B)} \quad (3)$$

where P (A | B) is a possibility in the case of when B occurs, A occurs.

4.2.4 Rule - DTNB

DTNB [35] investigates a simple semi-naive Bayesian ranking method that combines naive Bayes with an induction of decision tables. Naive Bayes and decision tables can both be trained efficiently, and the same holds true for the combined semi-naive model.

4.2.5 Meta – Bagging

Bagging [36] predictors is a method for generating multiple versions of a predictor, with which to construct an aggregated predictor. The aggregation averages over the versions when predicting a numerical outcome, and triggers a plurality vote when predicting a class. The multiple versions are created by bootstrapping duplications on the learning set, and then using these versions as new learning sets. The authors of [36] tested real and simulated data sets by utilizing classification and regression trees. Its subset selection with a linear regression shows that bagging can substantially gain in accuracy.

Although the Decision tree, rules and Bayes shown in Table 3 obtain good accuracies, decision tree is simpler, and has less computation. Therefore, we choose it as the classification mechanism.

4.3 Our Classification Tool

Figure 3. The decision tree obtained by inputting our experimental results listed in the Appendix of this Chapter to the Weka.

According to Table 2, we put the experimental result data, collected by using the Triaxial accelerometer and gyroscope and shown in Appendix of this chapter, into weka and obtain the Decision Tree shown in Figure 3.

Firstly, a threshold value is 2.1g on SMV is chosen. If the SMV value is less than the threshold, we consider that the corresponding body movement is an ADL, which may be standing up (when the minimum of Pitch is smaller than or equal to -11.9 degrees), walking (when the minimum of Pitch is larger than -11.9 degrees and the maximum of Pitch is smaller than or equal to 24.4 degrees) or sitting down (when the Pitch is larger than -11.9 degrees and the maximum of Pitch is larger than 24.4 degrees). Otherwise, it is a falling or running. When the minimum of Pitch is smaller than or equal to -40.1 degrees, it is a body turning left when falling backward (when the

maximum of Roll is larger than 23.4 degrees) or a body turning right while falling backward (when the minimum of Roll is smaller than or equal to -20.9 degrees). When the minimum of Roll is larger than -20.9 degrees, the movement is a falling backward. When SMV is larger than 2.1g, the minimum of Pitch is larger than -40.1 degrees and the maximum of Pitch is larger than 57.4 degrees, it is a falling forward. Otherwise, it is a falling right (when minimum of Pitch is larger than -40.1degree, the maximum of Pitch is smaller than or equal to 57.4 degrees and the maximum of Yaw is larger than 50.7 degrees) or Running (when the maximum of Yaw is smaller than or equal to -50.7 degrees and minimum of Yaw is larger than -66.2 degrees). If the minimum of Yaw is smaller than or equal to -66.2 degrees, it is a falling left.

TUNGHAI UNIVERSITY COMPUTER SCIENCE DEPARTMENT
1981
東海大學
資訊工程學系

5. Evaluation

In this section, we use the data collected by using Triaxial accelerometer and gyroscope to analyse the accuracy of the Decision Tree generated by the Weka. First, we classify a movement into a falling or one of the four types of mentioned ADL. In the first experiment, we discriminate whether it is a fall or an ADL. If it is an ADL, the movement is then further classified it into sitting down, standing up, walking or running, identified as Fall and ADL-classes (F-ADL-class) classification. In the second experiment, a movement is classified into one of the six types of mentioned falling or one of the four types of chosen ADL, denoted by movement (M-class) classification.

During the experiments, we place a smart phone on the user's chest. In order to eliminate additional confounding variables, and bring the experiments closer to their ideal states, we strap the phone parallel to the chest so that the measurement of acceleration of gravity can be closer to the body's value. This may relatively be free from interference of other external factors.

5.1 Ceiling effect

In our previous study, when the acceleration of gravity of iPhone 4 is greater than 3.5g, the ceiling phenomenon as shown in Figure 4 appears, even the Apple claims that iPhone4 can measure more than 4g of gravity [37]. We first test the Apple products, including iPhone 4 – iPhone 6 and compare their performance.

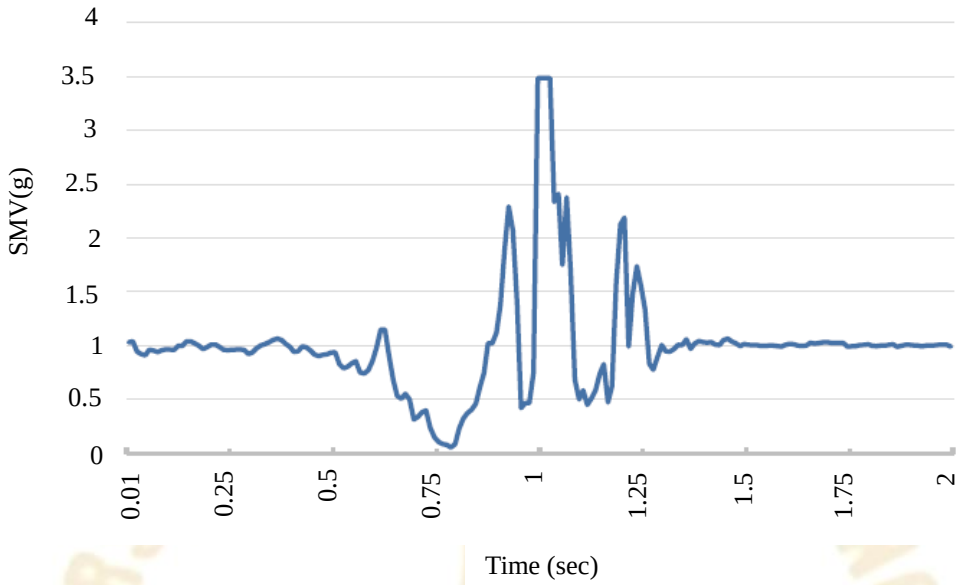

Figure 4. Ceiling phenomenon on iPhone4.

The Triaxial accelerometer chips for the three iPhones models are shown in Table 4 [37][38][39][40].

The experimental results are shown in Figure 5, in which the three models measure the similar values when the gravity is smaller than 3g. When the acceleration of gravity is higher than 3g, the ceiling phenomenon of iPhone4 appears. But this time its acceleration cannot be larger than 3.2g. We can see iPhone5 and iPhone6 can measure up to 9g,

Table 4. The generations of iPhone of triaxial accelerometer chip.

Product	iPhone 4	iPhone 5	iPhone 6	
Brand	STMicroelectronics	Bosch	Bosch	Inven Sense
Model	LIS331DLH [37]	BMA220 [38]	BMA280 [39]	MPU-6500 [40]
Measurement Range	±2.0 ±4.0 ±8.0	±2.0 ±4.0 ±8.0 ±16.0	±2.0 ±4.0 ±8.0 ±16.0	±2.0 ±4.0 ±8.0 ±16.0

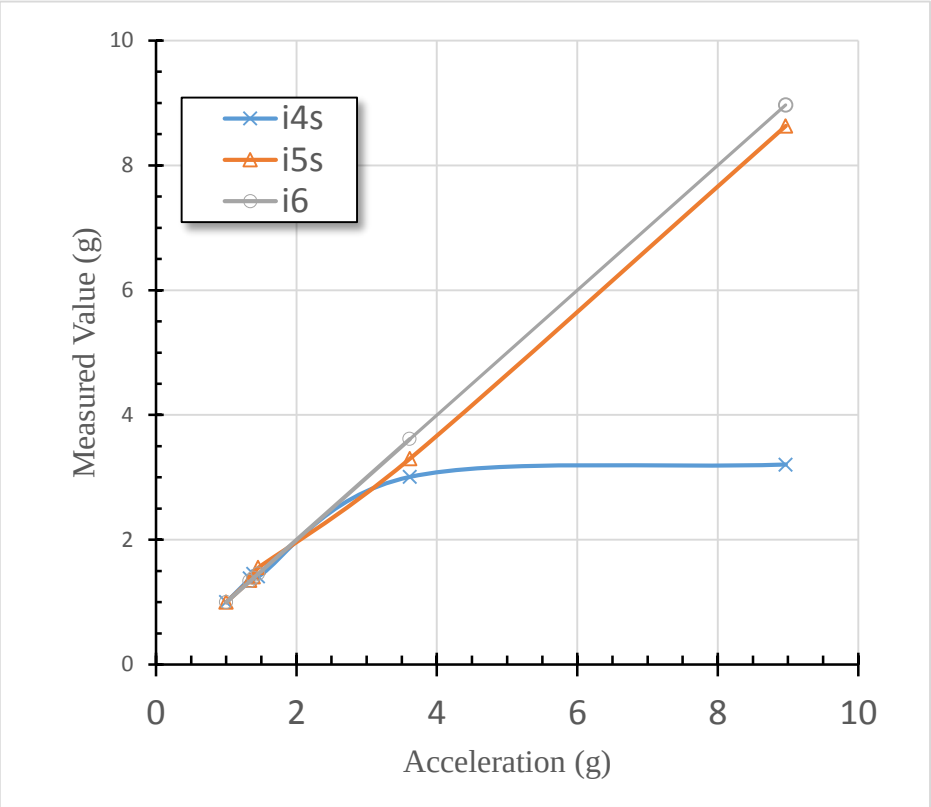

Figure 5. Measured values of Triaxial accelerometer for three iPhone models, including iPhone4-iPhone6.

5.2 Evaluation Criteria

As shown in Table 5, the precision of F-ADL-class classification was 98.5%, and its recall was 98.5%. The precision of M-class classification was 97.2%, and its recall was 96.5%. Precision and Recall as our test metrics are defined as follows.

$$\text{Precision} = \frac{\text{TP}}{TP+FP} \tag{4}$$

and

$$\text{Recall} = \frac{\text{TP}}{\text{TP+FN}} \tag{5}$$

where TP standing for true positives is defined as a fall occurs and the detection system accurately discovers it. FP standing for false positives is defined as that the detection system announces that there is a fall, but actually, it is not a fall. TN standing for true negatives is defined that as it is a non-fall movement, and the system classifies the movement as an ADL. Moreover, FN standing for false negatives is defined as that a fall occurs, but the system classifies it as an ADL.

Table 5. Accuracies of F-ADL-class classification and M-class classification (%)

Classification	Accuracy	TP	FP	FN	Precision	Recall	F-measure
F-ADL-class classification	98.5	98.5	2	2	98.5	98.5	98.4
M-class classification	96.5	96.5	0.4	3.5	97.2	96.5	96.8

F-measure as a metrics taking into account both precision and recall is applied to assess the effectiveness of information retrieval [41], and is defined as:

$$\mathrm{F}_{\mathrm{measure}} = \frac{2}{\left(\frac{1}{Precision}+\frac{1}{Recall}\right)} = \frac{2\times Precision\times Recall}{(Precision+Recall)}$$

$$= \frac{2\times TP}{(2\times TP+FP+FN)} \quad (6)$$

Accuracy of determining whether there is a fall or it is an ordinary ADL on movements in F-ADL-class classification is 98.46%. However, after further classifying fallings, the accuracy of M-class classification is reduced to 96.57%.

Table 6 is the confusion matrix of F-ADL-class classification, in which only one running was misclassified to falling. The reason is that it is a discontinuous jump with

a greater gravity, and is then prone to false positives.

Table 6. The confusion matrix of F-ADL-class classification.

The FDSMP classification / Actual classification	Walking	Running	Sitting down	Standing up	Falling
Walking	50	0	0	0	0
Running	0	49	0	0	1
Sitting down	0	0	50	0	0
Standing up	0	0	0	50	0
Falling	0	0	0	0	150

Table 7 is the confusion matrix of M-class classification, in which the miscarriage of justice appears at the judgment of falling right and falling left movements, mainly because the two falls are not simple ones. They could be a falling left (right) and tumbling down to the left (right) at the same time. They are prone to the false positives. From F-ADL-class classification and M-class classification, we found that the accuracy of determining whether there is a fall without falling classification or not or the movement is an ordinary ADL (with further ADL classification) is high. However, when detecting the movement of falls, the situation in reality is not that simple like our classification, e.g., it is possible that falling right and turning to the left are performed at the same time, causing a large gravity in the SMV, consequently leading to high difficulties in correct falling judgment and ADL classification.

Table 7. The confusion matrix of M-class classification.

Actual classification \ The FDSMP classification	Walking	Running	Sitting down	Standing up	Falling Forward	Falling Backward	Falling Right	Falling Left	Body turning right while falling backward	Body turning left while falling backward
Walking	50	0	0	0	0	0	0	0	0	0
Running	0	49	0	0	1	0	0	0	0	0
Sitting down	0	0	50	0	0	0	0	0	0	0
Standing up	0	0	0	50	0	0	0	0	0	0
Falling Forward	0	0	0	0	25	0	0	0	0	0
Falling Backward	0	0	0	0	0	25	0	0	0	0
Falling Right	0	0	0	0	0	0	24	0	1	0
Falling Left	0	0	0	0	0	0	0	24	1	0
Body turning right while falling backward	0	0	0	0	0	1	0	0	24	0
Body turning left while falling backward	0	0	0	0	0	0	0	0	0	25

5.3 Signal Analysis

The signals including Triaxial accelerations and gyroscope angles collected for different movements are comprehensively compared and analyzed. Bruno *et al.* [22] also analyzed signals for falls. The actions of a fall can be divided into three phases, i.e., free falling, the body stroking the floor and the body staying lying. We also record the actions of a fall with a video, besides the data collected by using gyroscope/Triaxial accelerometer, so that we can identify the correspondences between an action and its recorded signals.

The four types of our chosen ADLs are mainly distinguished by Pitch (see the left subtree of Figure 3). In fact, the Roll and Yaw are the body's natural swing, produced by the control of body center of gravity. They do not constitute an important basis in ADL movement analysis. The time interval for the FDSMP to

access the acceleration values and the angle variation is 0.01 second.

The six types of falling need to distinguish by the three-axes values of the gyroscope. As mentioned above, falling is usually accompanied by other fall patterns, and therefore, cannot be simply classified. The compound falling activities appear mainly because of the body's self-protection actions and instability control of the center of gravity. The purpose is to reduce the physical injury caused by the falling. In these actions, body is often curled or tumbled even simultaneously.

TUNGHAI UNIVERSITY COMPUTER SCIENCE DEPARTMENT
1981
東海大學
資訊工程學系

5.3.1 Standing Up

The signals we record for standing up, including its SMVs, Triaxial accelerations and gyroscope angles, are shown in Figure 6. Before standing up, we need to bend our upper bodies to move the center of gravity forward. Figure 6b shows that the experimental Pitch is about 23 degrees of ups and downs, and that the Roll and Yaw have only a slight rotation around the body. But due to different weight transfers and personal habits, different people may present different results. However, the difference in results is often small. Comparing Figure 6a and 6b, it can be seen when the body leaned forward the maximum, the SMV goes up and the peak is about 1.7g. In Figure 6c, y-axis starts at -1g, because the gravity of earth is in the negative direction of y-axis. When his/her buttocks leave the chairs, there is a smooth peak and an acceleration goes upward, causing the Triaxial acceleration on y-axis to be about -1.6g. While the user bends over, the gravity of earth shifts a portion to the positive direction of z-axis. That is why acceleration on z- axis increases.

東海大學
資訊工程學系

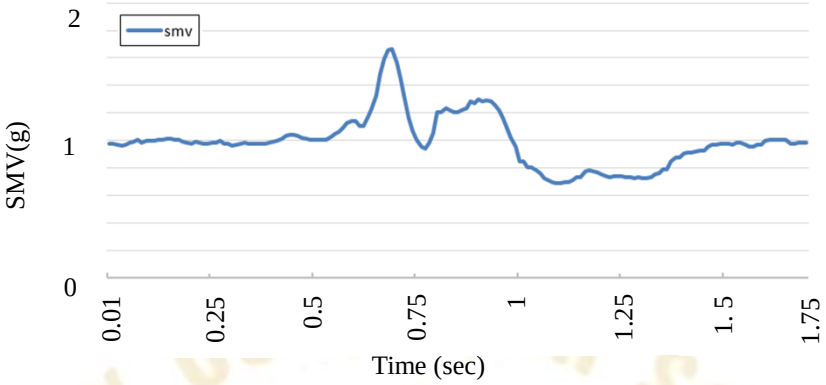

(a) SMVs of a Standing Up

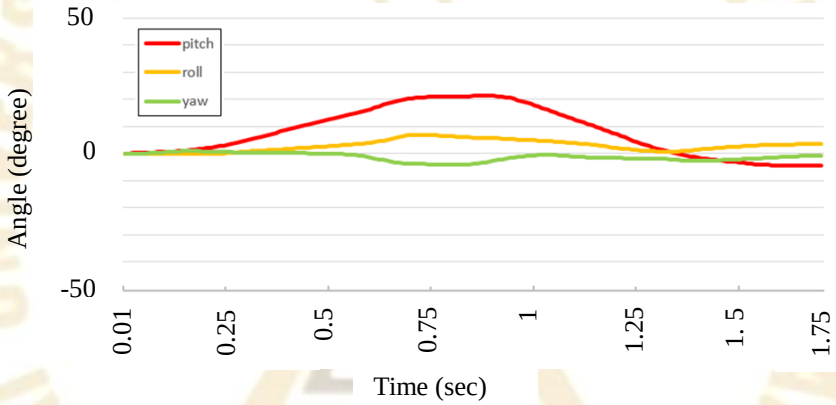

(b) Gyroscope angles including Pitch, Roll and Yaw of standing up

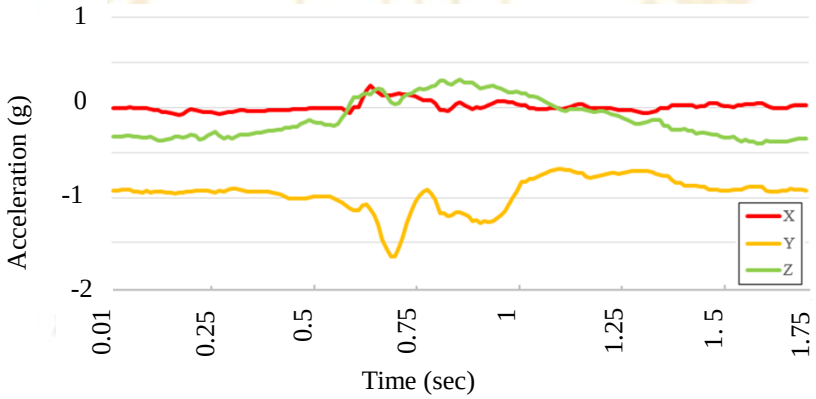

(c) Accelerations of standing up

Figure 6. The SMVs, accelerations and Gyroscope angles on a standing-up movement.

5.3.2 Sitting down

Before sitting down, we also bend over to move the center of body gravity forward to balance our body. The SMVs, Triaxial accelerations and gyroscope angles, are plotted in Figure 7. In Figure 7b, the maximum of Pitch is about 45 degrees, meaning the upper body bends over 45 degrees. The angles of Roll and Yaw are relatively small. In Figure 7c, we can also see that gravity of y-axis is negative due to gravity of earth. When his/her body starts moving downward, y-axis has a smooth peak, which is about -0.5g. When the user bends over, like that on standing up, the gravity of earth shifts a part to the positive direction of z-axis. That is why the acceleration in z-axis increases.

TUNGHAI UNIVERSITY COMPUTER SCIENCE DEPARTMENT
1981
東海大學
資訊工程學系

(a) SMVs of sitting down

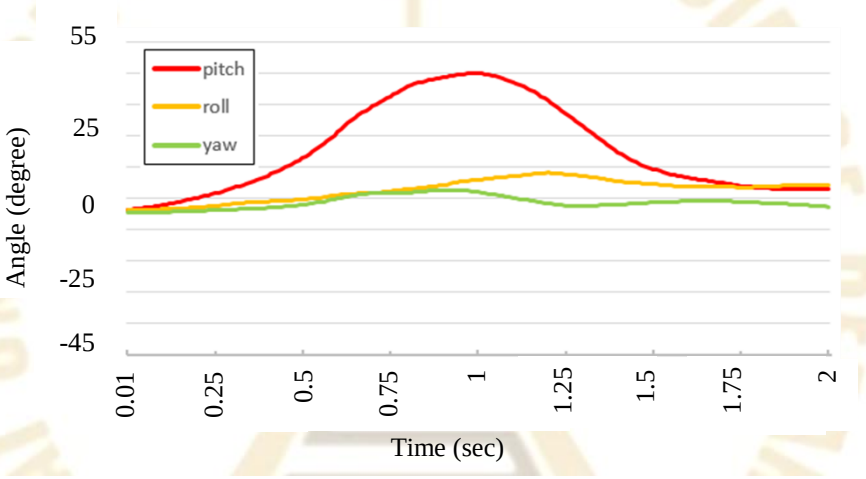

(b) Gyroscope angles including Pitch, Roll and Yaw of sitting down

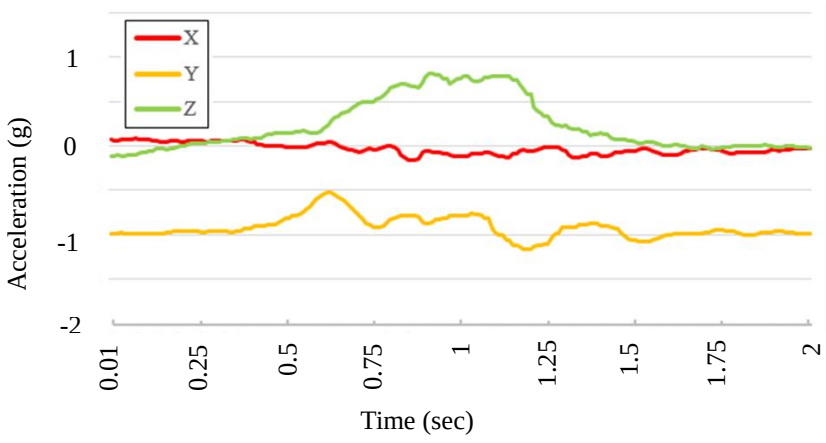

(c) Accelerations of sitting down

Figure 7. The SMVs, accelerations and gyroscope angles on sitting down movement.

5.3.3 Walking

Walking and running are movements with cyclical characteristics. So we can observe all steps of them. The recorded SMVs, Triaxial accelerations and gyroscope angles, are shown in Figure 8, which illustrates that the user walked a total of 6 steps, and from which we can see the ups and downs of Pitch on each step. In Figure 8, each rectangle contains the signals of a step. Although we do not obviously feel the change of Pitch of the body while walking, we can see the second and third portraits shown in Figure 9a from the left. When our legs stretch forward, body will slightly tilted forward to balance the center of body gravity.

In Figure 9b, when the user moves his/her left foot forward, as that in the second rectangle, the corresponding Roll is positive, which comes from the fact that his/her buttocks turn to right (see the first portrait in Figure 9b), but his/her chest turns left a little to balance the center of body gravity, resulting in a small positive for Roll. Figure 9b also shows that when the user steps out the right foot, similarly the buttocks will rotate to the left. But the chest will turn right a little. So in the first rectangle in Figure 8b, Roll goes down, meaning chest turns right. Of course, when his/her buttocks turn left, meaning he/she stretches his/her right leg, Roll has a small rotation in its negative direction.

Now it is easy to recognize which leg the user stretches in the second rectangle, Roll goes up, indicating that he/she moves his/ her left leg forward. Figure 9c illustrates that while walking, our upper bodies will slightly vibrate along z-axis, generating Yaw angles (see the second and fourth portraits). But different persons have different movement styles. In Figure 8b, the Yaw almost remains unchanged. In Figure 8a, each step has 2 peaks in SMV, mainly resulting from the shake of

accelerations in y-axis and z-axis. The first peak occurs when a foot touches the ground, which causes an acceleration in negative y-axis. The second peak is resulted from the body moving forward. The acceleration of gravity shifts a portion to the positive direction of z-axis as the acceleration in that axis.

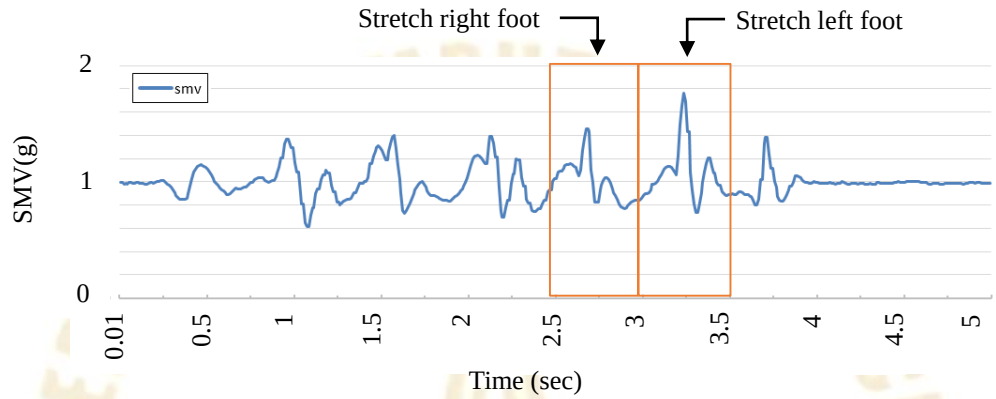

(a) SMVs of Walking

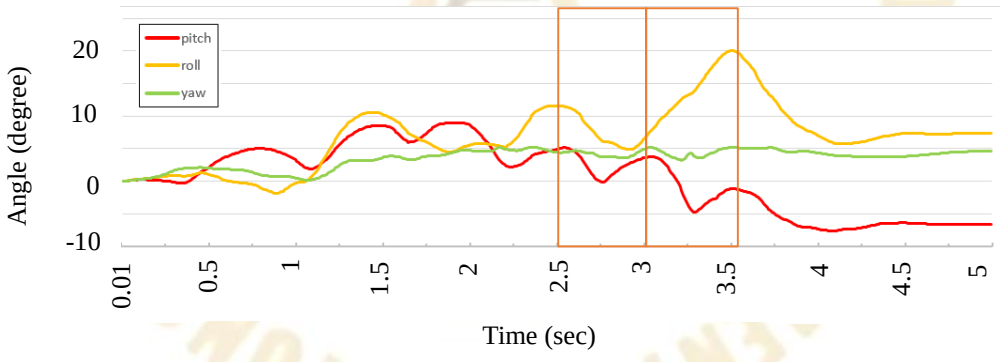

(b) Gyroscope angles including Pitch, Roll and Yaw of walking

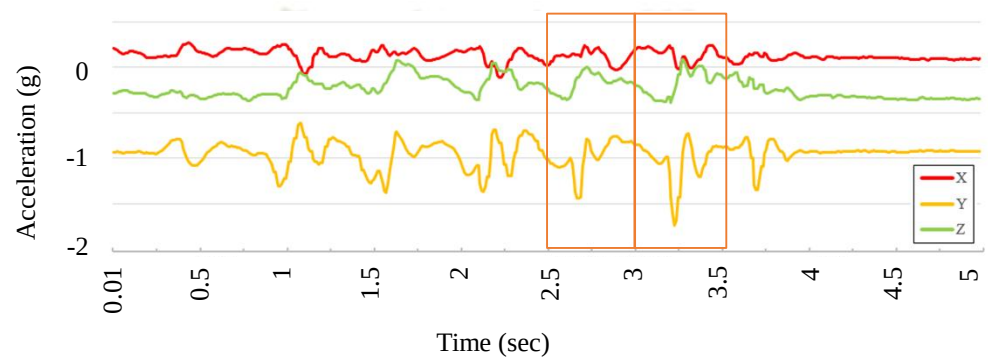

(c) Accelerations of walking

Figure 8. The SMVs, accelerations and gyroscope angles on walking movement.

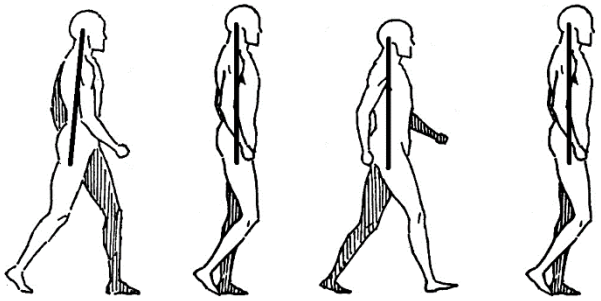

(a) Side look of Walking

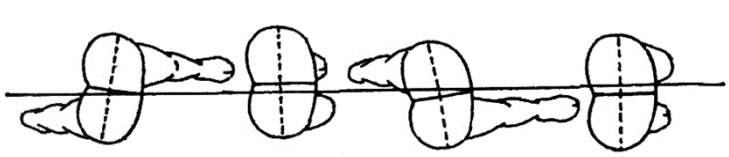

(b) Overlook of Walking

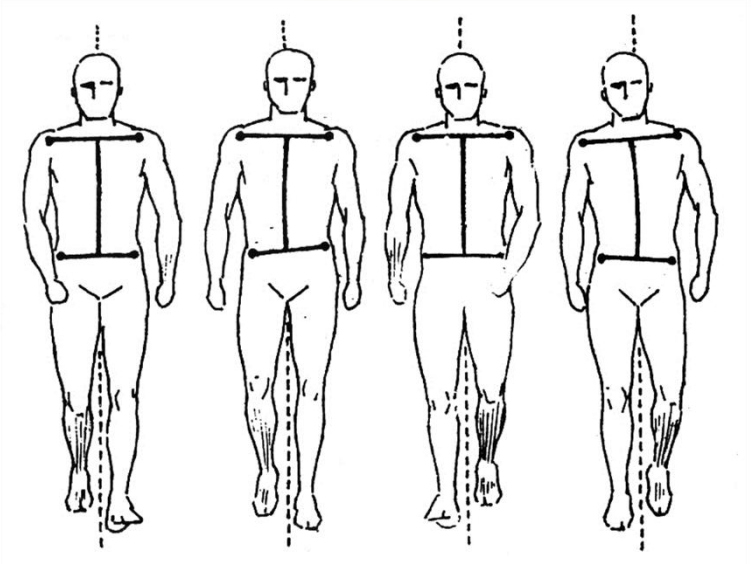

(c) Front look of Walking

Figure 9. Schematic of Walking [42].

5.3.4 Running

Figure 10 illustrates the recorded SMVs, Triaxial accelerations and gyroscope angles for the person who ran a total of 10 steps. Like that in Figure 8, each rectangle contains signals of a step. Running can be regarded as a jumping forward. At the beginning of running, like that of walking, we often bend over our upper bodies for the first step. The maximum of Pitch measured is about 19 degrees. In the first rectangle, since Roll goes up, it means that the person stretches his/her left leg for running. Of course, the signals contained in the second rectangle is generated when he/she stretches his/ her right leg. In Figure 10c, we can see that because of the swing of the body, the acceleration of x-axis has a small peak about 2g. On each step, when a foot touches the ground, an acceleration about -2.5g in y-axis is measured.

東海大學
資訊工程學系

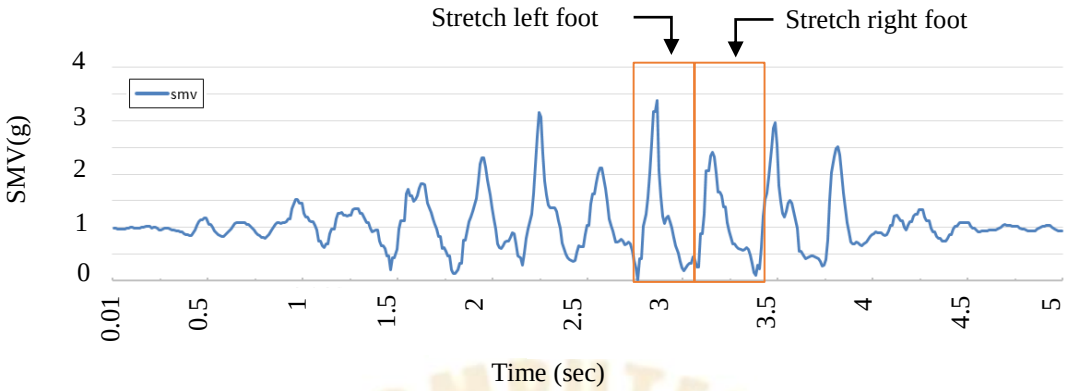

(a) SMVs of a running

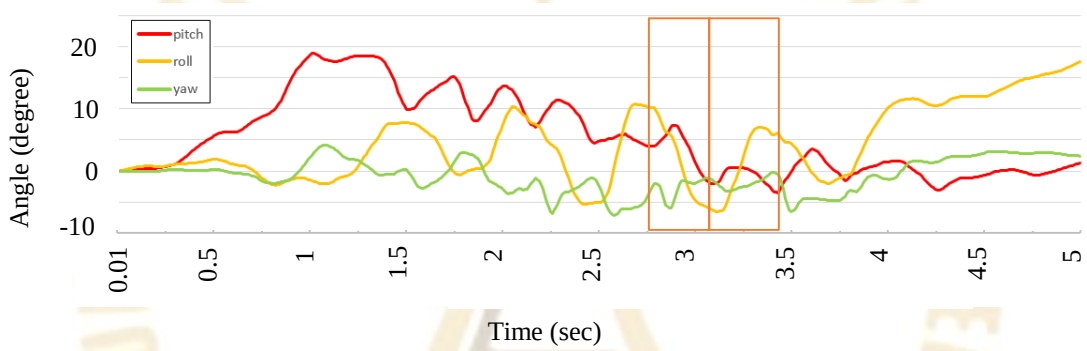

(b) Gyroscope angles including Pitch, Roll and Yaw of a running

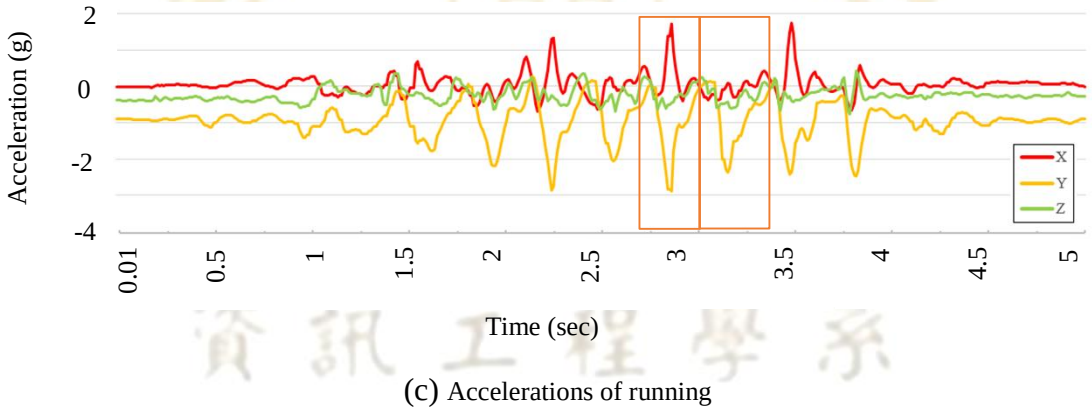

(c) Accelerations of running

Figure 10. The SMVs, accelerations and gyroscope angles on a running movement.

5.3.5 Falling Forward

In the following, falling experiments will be performed, and the generated signals will be analyzed. The entire falling process is also recorded by a video recorder.

Figure 11 plots the SMVs, Triaxial accelerations and gyroscope angles for falling forward. In Figure 11a and 11b, the time period on the left of the red bar is free falling. The first peak of SMV, as the indicated 1, is the impact when knees hit the ground. There is an acceleration toward to the ground (see y-axis in Figure 11c). There is also a peak in z- axis, indicating that there is a z-axis acceleration, i.e., the body is still forwarding. The second peak, as the indicated 2, is generated when the palms touch the ground. In Figure 11c, there is a small peak in x-axis, which means the user's right hand touches the ground before his/her left hand does, causing an acceleration on negative direction of x-axis, and z-axis acceleration still exists. The latter results in another peak in z-axis.

The last peak, as the indicated 3, is formed when the body collides with the ground. There is a peak in y-axis which is almost overlapped with the peak in z-axis. Because when touching the ground, his/her body continues going forward in the y-axis. The two small peaks between 1 and 2 and between 2 and 3 are created by the rebound of the phone in the user's pocket. When the body hits the ground (number 3), because the device is under pressure of the body, the strength of the impact is the largest with no rebound of the phone. Figure 11c clearly shows that the three peaks are most dominated by the z-axis.

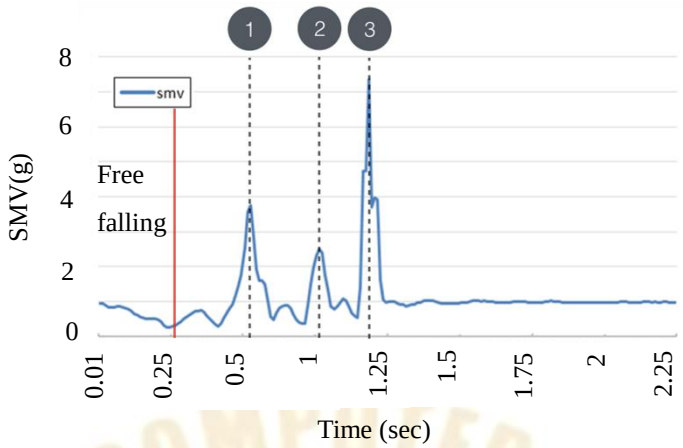

(a) SMV of falling forward

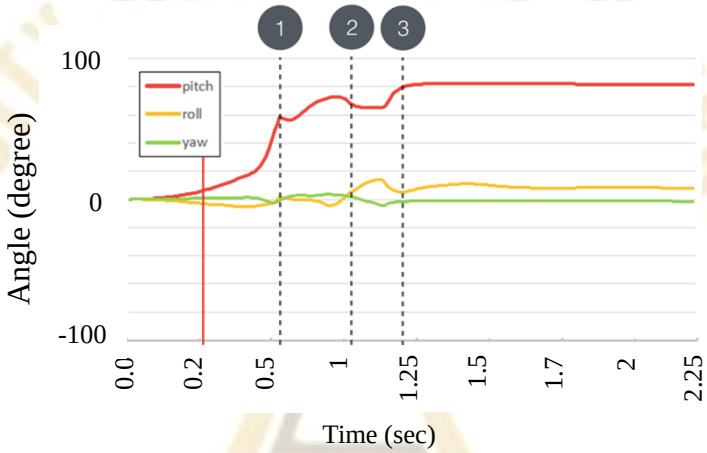

(b) Gyroscope angles including Pitch, Roll and Yaw of falling forward

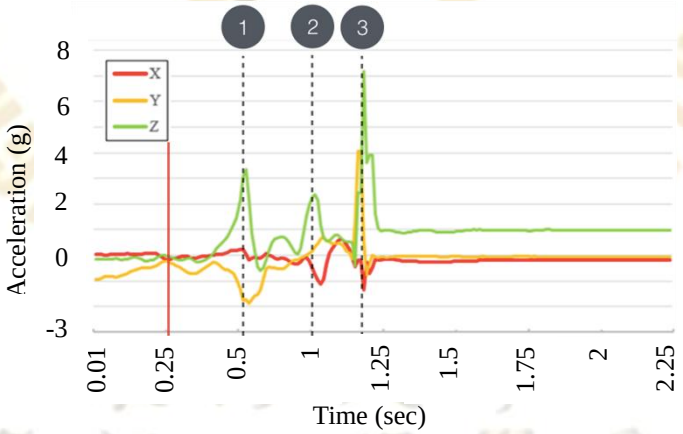

(c) Accelerations of falling forward

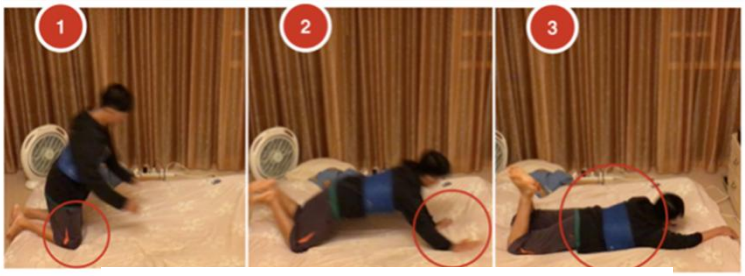

(d) The pictures recorded by video recorder

Figure 11. The SMVs, accelerations and gyroscope angles on falling forward movement.

5.3.6 Falling Backward

Figure 12 plots the SMVs, Triaxial accelerations and gyroscope angles for falling backward. In Figure 12a and 12b, like those in Figure 11, the time period on the left of the red bar is free falling. The first peak of SMV, as the indicated 1, occurs when the person curled up the body forward in order to slow the speed of the falling so as to reduce body injury. The Pitch is then positive. The second peak, as the indicated 2, is generated when the buttocks hit the ground, forming the largest impact. The last peak, as the indicated 3, occurs when the user tries to balance his/her body, but failed at the end. Finally, user's head and body touch the ground.

After the maximum of the peak (between 2 and 3), there are several small peaks, which are produced by the rebound of the phone in the user's pocket. In Figure 12b, Pitch between 1 and 2 goes down since user's upper body gradually moves backward, and at last becomes negative. Its final angle is about -80 degrees. Roll and Yaw almost remain unchanged. In Figure 12c, we can see the second peak is produced by the accelerations in y-axis and z-axis. The biggest is that in y-axis, because the body (buttocks) hits the ground vertically. We know that it probably causes injury of vertebral. In z-axis, when the person's body hits the ground, there is an acceleration backward which is negative. It is clear that at this time point, the acceleration in negative z-axis is high. It is also the reason why the person's body continues moving backward. We can also see the acceleration in x-axis at 3 fluctuates. This is because when user's body hits the ground, his/her left shoulder touches the ground first (positive x-axis) and then the right shoulder (negative x-axis). At 3, there is also a small peak in negative z-axis, meaning that when the user's head and body touch the ground, the impact is not serious.

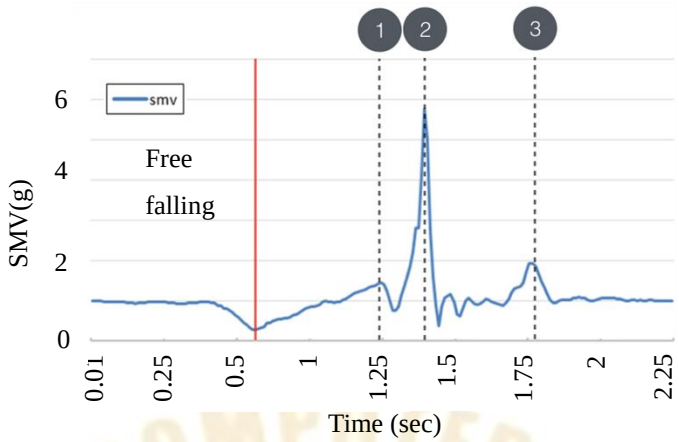

(a) SMVs of falling backward

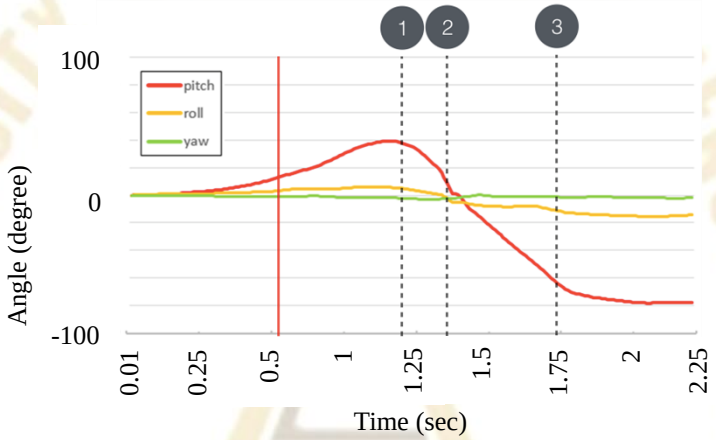

(b) Gyroscope angles including Pitch, Roll and Yaw of falling backward

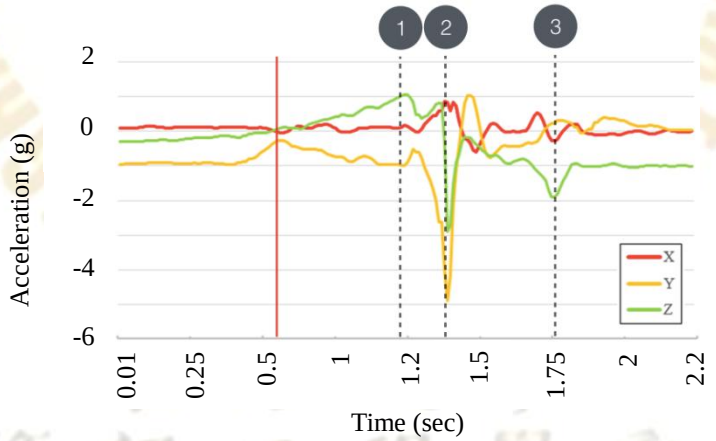

(c) Accelerations of falling backward

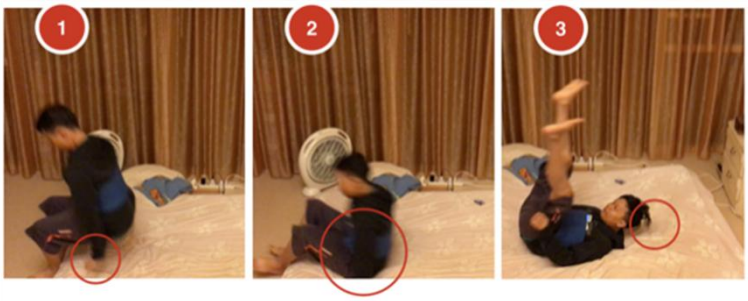

(d) The pictures recorded by video recorder

Figure 12. The SMVs, accelerations and gyroscope angles on falling backward movement.

5.3.7 Falling Right

Figure 13 illustrates the SMVs, Triaxial accelerations and gyroscope angles of a falling right. Before the maximum of the peak shown in Figure 13a, Pitch shown in Figure 13b, is positive, which is about 15 degrees since the user curls up his/her body forward in order to slow the falling speed so as to reduce body injury. The maximum of the peak is produced when the user's buttocks hit the ground. Roll is about +15 degrees since the user turns his/her body left a little, and uses his/her right-hand elbow to touch the ground in order to mitigate falling injury. Yaw at last is about +120 degrees. As shown in Figure 13a, the SMV peak is about 6g, which as shown in Figure 13c is created by the acceleration of the three-axes. The acceleration in x-axis is about -3g. It is negative because the body hits the ground rightward, and rightward is the negative direction of x-axis. The acceleration in y-axis is about -3g. which is negative because of falling down. The acceleration in z-axis is about 4g. Because the user tries to touch the ground with his/her right-hand elbow, and the body turns forward a little. That is why during the maximum impact, Roll goes down.

After the maximum impact, there are several moderate peaks (in Figure 13a, they are circled). They are generated due to the body hitting the ground. The acceleration in x-axis is about -2g. It is negative because the body hits the ground rightward. The acceleration in y-axis is about 0.5g, which is positive because the user's body is still moving toward his/her head direction. The acceleration in z-axis is about 1g because the user's right-hand elbow is still trying to relief the impact of his/her body with the ground. But at this moment, the acceleration is smaller.

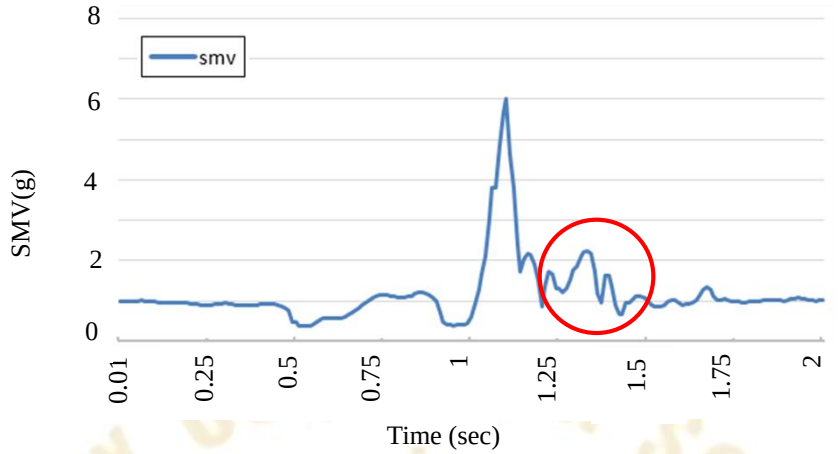

(a) SMVs of falling right

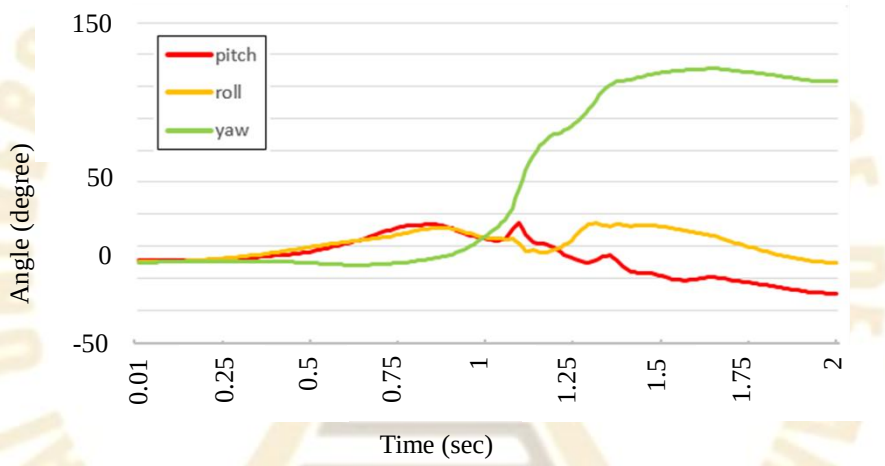

(b) Gyroscope angles including Pitch, Roll and Yaw of falling right

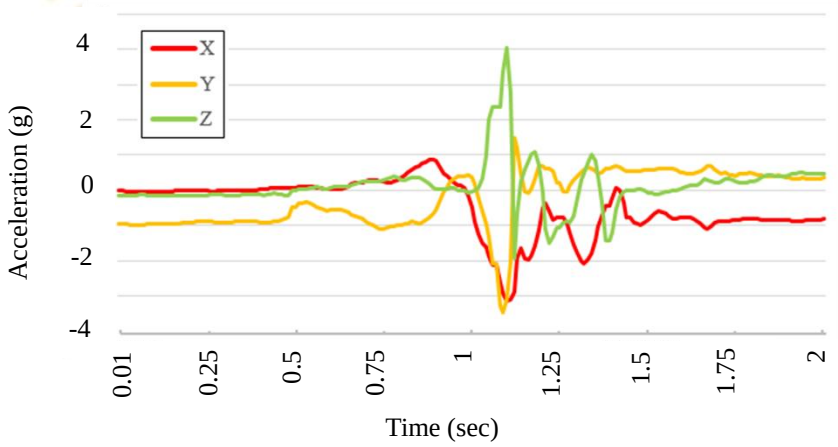

(c) Accelerations of falling right

Figure 13. The SMVs, accelerations and gyroscope angles on falling right movement.

5.3.8 Falling Left

Figure 14 illustrates the SMVs, Triaxial accelerations and gyroscope angles of a falling right. Before the maximum of the peak shown in Figure 14a, , Pitch as shown in Figure 14b is positive, which is about 25 degrees since the user curls up his/her body forward in order to slow the falling speed and reduce his/her body injury. The maximum of the peak shown in Figure 14a is produced when the user's buttocks hit the ground. The SMV is about 4.8g. Roll is about -20 degrees, meaning that the user turns the body a little rightward and uses his/her left-hand elbow to touch the ground in order to reduce falling injury. Yaw is about -40 degrees, which is negative since this is a falling leftward. As shown in Figure 14c, the maximum of the peak is created by the acceleration in three axes. The acceleration in x-axis is about 2.5g, which is positive because the body hits the ground leftward. The acceleration in y-axis is about -3.9g, which is negative because of falling down. The acceleration in z-axis is about 2g, which is positive because when the body touches the ground, the user turns his/her body a little forward. After the maximum impact, there is a circled peak shown in Figure 14a, which is created when the body hits the ground. The acceleration in x-axis is about 3.5g, which is positive because the user's body hits the ground leftward. The acceleration in y-axis is about 0.5g, which is positive because the user's body continues going toward his/her head direction (The positive direction of y-axis). The acceleration in z-axis is about 1g. It is because the body turns a little forward. The acceleration of gravity shifts a portion to positive direction of z-axis.

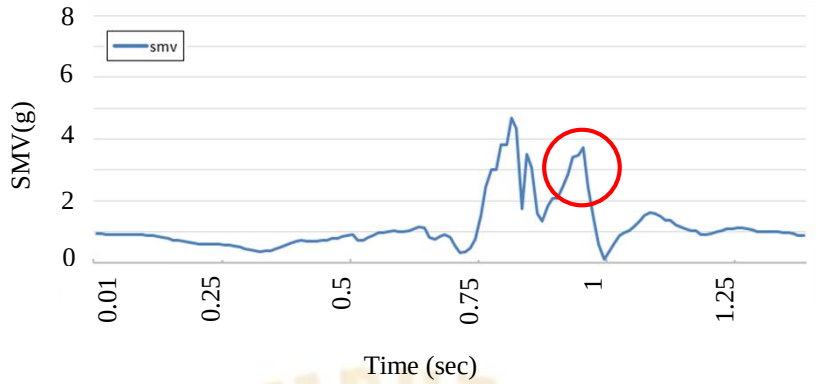

(a) SMVs of falling left

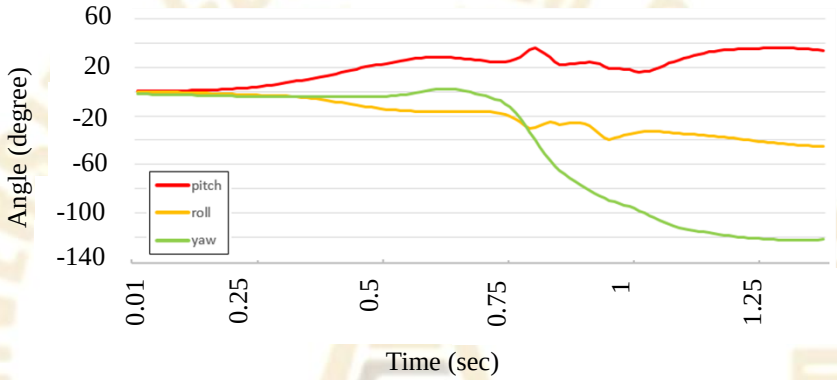

(b) Gyroscope angles including Pitch, Roll and Yaw of falling left

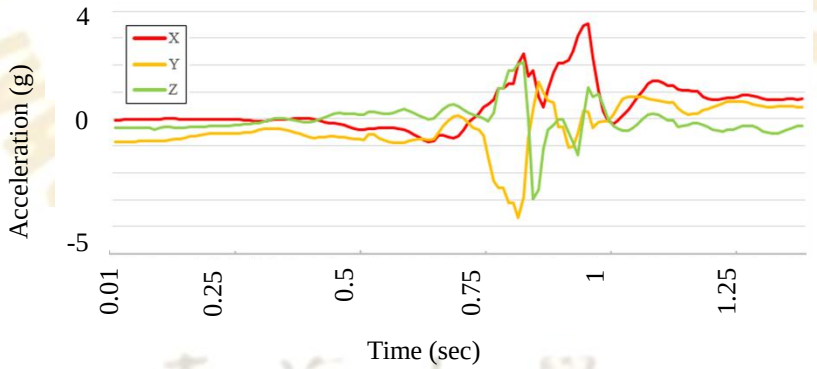

(c) Accelerations of falling right

Figure 14. The SMVs, accelerations and gyroscope angles on falling left movement.

5.3.9 Body Turning Right while Falling Backward

Figure 15 plots the SMVs, Triaxial accelerations and gyroscope angles of a turning right while falling backward. Before the maximum of the peak shown in Figure 15b, Pitch is positive, which is about 10 degrees since the user curls up his/her body forward in order to slow the falling speed and reduce body injury. On the maximum of the peak, Roll is about -60 degrees. It is the time when his/her buttocks hit the ground. As indicated in Figure 15a, the SMV is about 7g, which as shown in Figure 15c, is formed from the accelerations in the three axes. The accelerations in x-axis is about -4g, which is negative because the body turns rightward before his/her body hits the ground. But the body continues falling down a little backward. That is why there is a negative acceleration in z-axis, which is -5.5g. The acceleration in y-axis is about -5.2g. It is negative because of falling down. Since before touching the ground, the body turns to rightward. Yaw is finally turned to 80 degrees. The circled peak is produced when the body hits the ground. Because the user tries to touch the ground with his/her right-hand elbow to reduce falling injury. The acceleration in x-axis is about -2g, which is negative because the body turns right before hitting the ground. The acceleration in y-axis is about 2g, which is positive because when the right side of body hits the ground, the user's body continues going toward his/her head direction. The acceleration in z-axis is about -2g. Because when touching the ground, the body is a little backward.

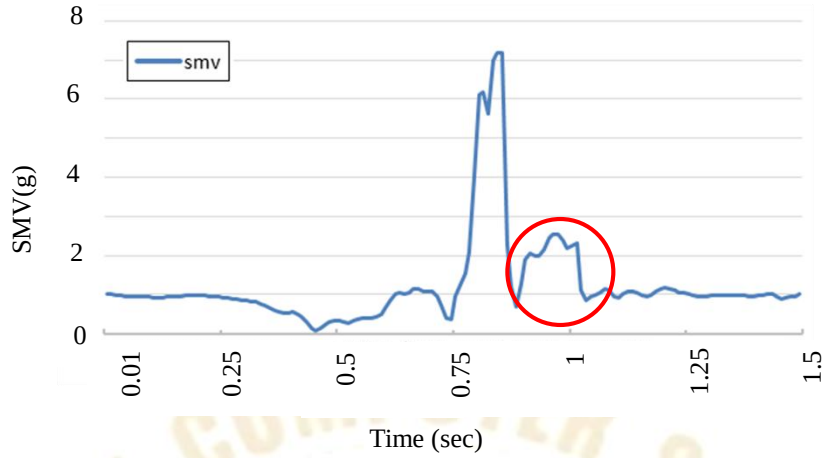

(a) SMVs of the body turning right while falling backward

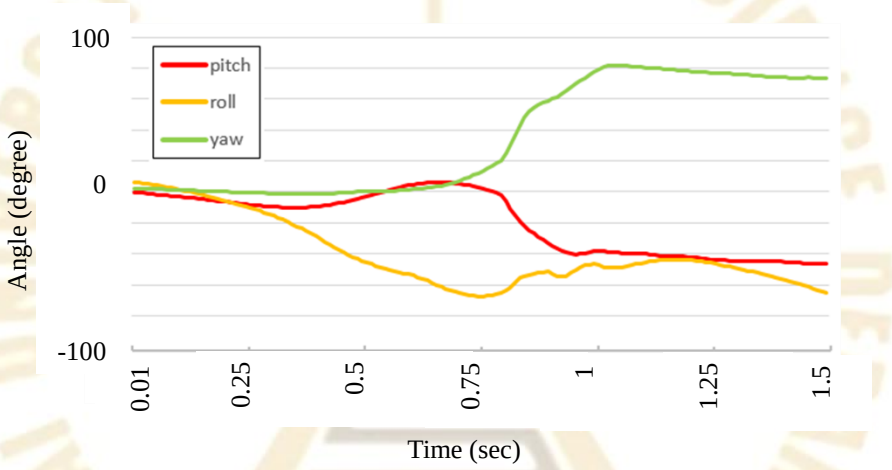

(b) Gyroscope angles including Pitch, Roll and Yaw on the body turning right while falling backward

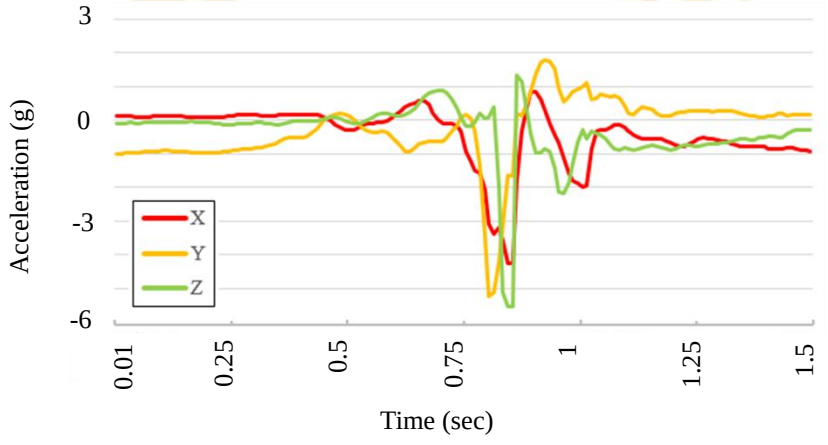

(c) Acceleration of the body turning right while falling backward

Figure 15. The SMVs, accelerations and gyroscope angles on the body turning right while falling backward movement.

5.3.10 Body Turning Left while Falling Backward

Figure 16 plots the SMVs, Triaxial accelerations and gyroscope angles of a turning right while falling backward. Before the maximum of the peak as shown in Figure 16b, Pitch is stable and almost 0 degree. Roll is about 40 degrees, which is positive since the user feels unsafe, and tries to turn leftward. The degree of the left turn is about 40. The peak SMC is produced when the buttocks hit the ground. As shown in Figure 16a, the SMV is about 7.9g. From Figure 16c, we can see the maximum of the peak is the combination of the three-axes accelerations. The acceleration in x-axis is about 4.8g, which is positive because the body turns to left and the buttocks hit the ground. The acceleration in y-axis is about -4.8g, which is negative because of falling down. The acceleration in z-axis is about -4.5g also due to falling backward. After the maximum impact, the body continues turning to left. At last, Yaw has turned to about -80 degrees. The circled peak is produced when the body hits the ground. The acceleration in x-axis is about 1g, which is positive because of the body turns to leftward and hits the ground. The acceleration in y-axis is about 1 degree. It is positive because when the body touches the ground, his/ her body is still going toward the positive direction of y-axis. The acceleration in z-axis is about -1. It is negative because of the falling backward.

東海大學
資訊工程學系

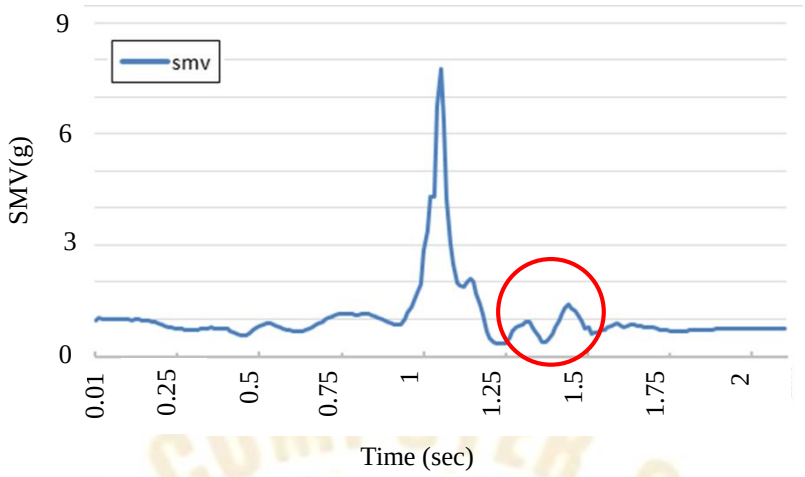

(a) SMVs of the body turning left while falling

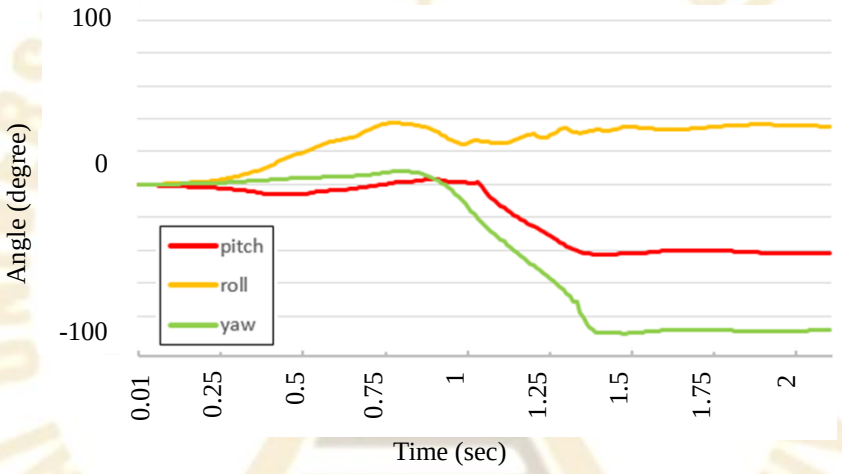

(b) Gyroscope angles including Pitch, Roll and Yaw of the body turning left while falling backward

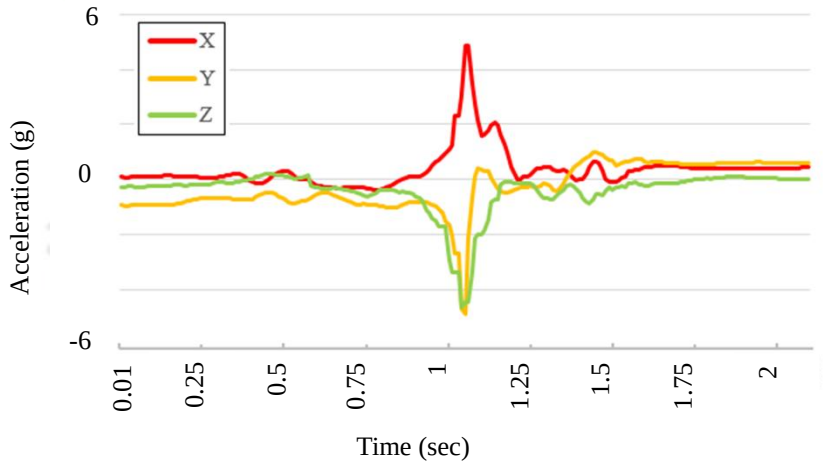

(c) Accelerations of the body turning left while falling backward

Figure 16. The SMVs, accelerations and gyroscope angles on the body turn left while falling backward movement.

6. Conclusions

As mentioned above, most of previous studies classified fallings by checking accelerations of gravity collected by Triaxial accelerometer. But only few of them use machine learning methods to enhance classification accuracy, while others employed a class of matrix-like complex mathematical operations. Only a few types of fall classification are involved. Nevertheless, the FDSMP more accurately classifies ADLs and the six types of fallings.

Nowadays, the sensing accuracy of triaxial accelerometer equipped in a phone is higher than before. When a new generation of mobile phones is released, the old data may often no longer useful, particularly for real time applications. So data need to be re-collected and re-calculated, before they can be used to judge whether it is an ADL or a falling. Although the process of re-collection and re-calculation is complicated, the accuracy is significantly improved.

Also many studies have shown that the use of machine learning will improve fall detection accuracies compared to those when only SMV thresholds are used. In this study, a total of nine machine learning methods are compared. We also analyze the data currently on hand. But a decision tree has a better analytical result than other machine learning methods. Especially the F-measure of J48 is the best among the night methods compared (shown in Table 3). Therefore, we adopt J48 to analyze the collected data.

From the above description, we found that if we use the gyroscope and Triaxial accelerometer simultaneously, the distinguish of fallings and ADLs can be more effectively and efficiently improved, and the identification of the direction of a fall can be also enhanced. In fact, a falling movement in reality is very complex, and is not so

idealistic like our study. Normally it is a mixture of several falling types, thus causing classification of falls to be very difficult in real world.

7. Future works and challenges

Currently, our preliminary data shows the superiority of our method. In the future, we will apply our experimental analysis to some complex information to further enhance our classification method. Some studies [4] mentioned that if we can send a multimedia messaging service and GPS coordinates telling caregivers to carry out the necessary relief work when an elderly falls, it will be more helpful to give the elder required help as soon as possible. We also like to explore other relevant technique to speed up fall detection.

Now a newly released smart phone can sense more objects and the accuracies are often higher than previous ones. Besides, many wearable devices are now more powerful than before. They can connect and transmit signals to mobile phones. In the future, we wish that a smart phone can also detect accidents, besides the elderly care, to make it really to be applied to medical applications and cares.

1981
東海大學
資訊工程學系

Reference:

[1] “World Population Ageing 2015 (Report),” United Nations,2015.

[2] “ Important Facts about Falls,” Centers for Disease Control and Prevention (CDC), September 21, 2015.

[3] “The Falls Management Program: A Quality Improvement Initiative for Nursing Facilities,” Agency for Healthcare Research and Quality, December 2012.

[4] C.Y. Ko, F.Y. Leu, and I-T Lin,” Using a smartphone as a track and fall detector: An intelligent support system for people with dementia,” Advanced Technological Solutions for E-Health and Dementia Patient Monitoring, 2015, pp. 272-295.

[5] M. V. Albert, K. Kording, M. Herrmann, A. Jayaraman, “Fall Classification by Machine Learning Using Mobile Phones,” PLOS One, May 7, 2012.

[6] Y.W. Bai, S.C. Wu and C.L. Tsai, “Design and Implementation of a Fall Monitor System by Using a 3-Axis Accelerometer in a Smart Phone,” IEEE Transactions on Consumer Electronics, 2012, pp1269-1275.

[7] Y. He, Y. Li, C.Yin, ”Falling-Incident Detection and Alarm by Smartphone with Multimedia Messaging Service (MMS),” E-Health Telecommunication Systems and Networks, 2012, pp. 1-5.

[8] T. Zhang, J. Wang, P. Liu and J. Hou, “Fall Detection by Embedding an Accelerometer in Cellphone and Using KFD Algorithm,” IJCSNS International Journal of Computer Science and Network Security, 2006, pp. 277-284.

[9] A.K. Bourke, J.V. O'Brien, G.M. Lyons, "Evaluation of a threshold-based tri-axial accelerometer fall detection algorithm," Gait Posture, 2007, pp.194-9.

[10] F. Spo sa, G. Tyson, "iFall: An android application for fall monitoring and response," 2009 Annual International Conference of the IEEE Engineering in Medicine and Biology Society, 2009, pp. 6119 – 6122.

[11] S.Y. Hwang, M.H. Ryu, Y.S Yang and N.B Lee, "Fall Detection with Three-Axis Accelerometer and Magnetometer in a Smartphone," Computer Science and Technology, 2012, pp. 65-70.

[12] C. Doukas, I. Maglogiannis, "Advanced Patient or Elder Fall Detection based on Movement and Sound Data," Pervasive Computing Technologies for Healthcare, 2008. PervasiveHealth 2008. Second International Conference, 2008, pp. 103-107.

[13] A.Z. Rakhman, , L. E. Nugroho, , Widyawan, Kurnianingsih, "Fall Detection System Using Accelerometer and Gyroscope Based on Smartphone," 2014 1st International Conference on Infonnation Technology, Computer and Electrical Engineering (ICIT ACEE) , 2014, pp. 99-104.

[14] J. Dai, X. Bai, Z. Yang, Z. Shen and D. Xuan, "PerFallD: A Pervasive Fall Detection System Using Mobile Phones," IEEE Int Conf on Pervasive Comp and Comm, 2010, pp. 292-297.

[15] N. Noury, A. Fleury, P. Rumeau, A. K. Bourke, G. Ó Laighin, V. Rialle, and J.E. Lundy,"Fall detection- Principles and Methodes," Annual International Conference of the IEEE Engineering in Medicine and Biology Society, 2007, pp.1663-1666.

[16] Q.Li, J. A. Stankovic, M. A. Hanson, A.T. Barth, J. Lach, G. Zhou, "Accurate, Fast Fall Detection Using Gyroscopes and Accelerometer-Derived Posture Information," 2009 Sixth International Workshop on Wearable and

Implantable Body Sensor Networks, Berkeley, CA, 2009, pp. 138-143.

[17] Y.S. Delahoz and M.A. Labrador, “Survey on fall Detection and Fall Prevention Using Wearable and External Sensors,” Sensors, 2014, vol. 14, Issue 10, pp. 19806-19842.

[18] N. El-Bendary, Q. Tan, F. C.Pivot, A. Lam, ” Fall Detection and Prevention for the Elderly: A Review of Trends and Challenges,” Int. J. Smart Sens. Intell. Syst, 2013, pp. 1230-1266.

[19] R. lgual, C. Meduano and I. Plaza,” Challenges, issues and trends in fall detection systems,”BioMedical Engineering,voi.10, 2013.

[20] Z. Zhao, Y. Chen, S. Wang, Z. Chen,” FallAlarm: Smart Phone Based Fall Detecting and Positioning System,” Procedia Computer Science, 2012, pp. 617-624.

[21] B. Aguiar, T. Rocha, J. Silva, I. Sousa,” Accelerometer-Based Fall Detection for Smartphones,” MeMeA 2014, 2012, pp. 480-485.

[22] B.S. Beauvais,” MyVigi : An Android Application to Detect Fall and Wandering,” The Sixth International Conference on Mobile Ubiquitous Computing, Systems, Services and Technologies, 2012

[23] S.H. Fang, Y.C.Liang, K.M. Chiu,” Developing a Mobile Phone-based Fall Detection System on Android Platform,” Computing, Communications and Applications Conference (ComComAp), 2012.

[24] Waldner, J.Baptiste. “Nanocomputers and Swarm Intelligence,” London: ISTE John Wiley & Sons. 2008.

[25] Penrose, Roger “17.4 The Principle of Equivalence,” The Road to Reality, New York, Knopf, pp. 393–394.

[26] “Gyroscope,” Oxford Dictionaries, Retrieved 4 May 2015.

[27] T.C. Smith, E. Frank, “Statistical Genomics: Methods and Protocols,” chapter

Introducing Machine Learning Concepts with WEKA, Springer, New York, NY, 2016, pp. 353-378.

[28] J.R. Quinlan, "Simplifying decision trees," International Journal of Man-Machine Studies, 1987, vol.27, no.3, pp. 221.

[29] G. Kaur, A.Chhabra, “Improved J48 Classification Algorithm for the Prediction of Diabetes,” International Journal of Computer Applications, Vol.98 , No.22, 2014, pp.0975– 8887.

[30] B. Hssina, A. Merbouha, H. Ezzikouri, M. Erritali, “A comparative study of decision tree ID3 and C4.5,” (IJACSA) International Journal of Advanced Computer Science and Applications, vol. 4.2, 2014.

[31] J. R. Quinlan, “C4.5,” Programs for Machine Learning. Morgan Kaufmann Publishers, 1993.

[32] X. Wu, V. Kumar, J. R. Quinlan, J. Fhosh, Q. Yang. H. Motoda, G.J. McLachlan, A. Ng, P. S. Yu, Z.H. Zhou, M. Steinbach, D.J. Hand, D/ Steinberg “Umd.edu - Top 10 Algorithms in Data Mining,” Knowl Inf Syst, 2008.

[33] E.Frank, I.H.Witten, “Generating Accurate Rule Sets Without Global Optimization,” CiteSeerX, 1998, pp. 144-151.

[34] M.G.Kendall, A.Stuart, J.K.Ord, “Kendall's advanced theory of statistics,” Probability Theory, Sampling Theory, 1994.

[35] M.Hall, E.Frank, “Combining Naive Bayes and Decision Tables,” Proceedings of Twenty-First International Florida Artificial Intelligence Research Society Conference, AAAI Press, Coconut Grove, Florida, USA, 2008, pp. 15-17.

[36] L. Breiman, “Bagging predictors. Machine Learning,” University of California, Berkeley, 1996, pp.123-140.

[37] “MEMS digital output motion sensor ultra low-power high performance 3-axes “nano” accelerometer,” STMicroelectronics, 2010.

[38] “BMA220 Digital, Triaxial acceleration sensor Data sheet,” Bosch, 2011.

[39] “BMA280 Digital, Triaxial acceleration sensor Data sheet,” Bosch, 2014.

[40] “MPU-6500 Register Map and Descriptions Revision 2.1” InvenSense, 2013.

[41] V. Rijsbergen,C. J,”Information Retrieval (2nd ed.),” London, Butterworths. ,1979.

[42] Y.S. Chang “2D 動畫原理與製作 ,” http://www.eric-web.shu.edu.tw/100_2D_animation.html

TUNGHAI UNIVERSITY COMPUTER SCIENCE DEPARTMENT
1981
東海大學
資訊工程學系

Appendix. Data generated during different movement experiments

Table A1 lists the data generated during different movement experiments. Columns 1-7 are data collected by mobile phones. Attribute “Maximum” is the maximum SMV calculated by using, Eq. (1). The input data is x, y and z accelerations measured by using Triaxial accelerometer. On the other hand, “Pitch_max”, “Pitch_min”, “Roll_max”, “Roll_min”, “Yaw_max” and “Yaw_min” are acquired as follows. First, Pitch, Roll and Yaw are retrieved from gyroscope and each of them is input to Eq. (2) to calculate A_t. From A_t for Pitch, we choose the maximum and minimum as the Pitch_max and Pitch_min, Roll_max and Roll_min, and Yaw_max and Yaw_min are obtained in the same way. Column 8, denoted by F-ADL, is the movement classification performed manually, which only contains a fall and one of the ADL movement, i.e., our F-ADL-class classification. The ADL movement includes sitting down, standing up, walking and running. The last column, denoted by “Move” is the classification including the 6 types of falling and 4 types of ADL. The data is then input to the data mining tool Weka to generate the decision tree shown in Figure 3.

Table A1. The data generated during different movement experiments.

Maximum	Pitch_max	Roll_max	Yaw_max	Pitch_min	Roll_min	Yaw_min	F-ADL	Move
1.590393	6.150832	16.7976	5.527333	-6.11412	-1.90108	-1.99837	Walk	Walk
1.764702	8.98486	20.09615	5.193512	-7.62536	-1.87813	0	Walk	Walk
1.582481	18.23732	4.91798	6.927872	-1.18663	-5.25291	-0.00378	Walk	Walk
1.294769	14.41367	15.46086	3.737733	0	-0.00231	-1.47686	Walk	Walk
1.477216	10.51984	13.02625	3.434221	-0.56477	-0.67597	-4.51993	Walk	Walk
1.281524	10.14396	11.27137	5.533572	-0.58927	-0.14793	-3.29732	Walk	Walk
1.394435	11.46371	14.00411	5.14988	0	-0.19198	-3.6133	Walk	Walk
1.336542	14.06495	8.059727	1.402276	-0.03621	-7.54555	-3.91412	Walk	Walk
1.417204	10.65668	0.09269	4.85889	0	-13.3531	-1.35264	Walk	Walk

Maximum	Pitch_max	Roll_max	Yaw_max	Pitch_min	Roll_min	Yaw_min	F-ADL	Move
1.011905	18.66328	6.343953	9.071375	0	-5.33749	-1.05222	Walk	Walk
1.465553	8.816695	15.24999	7.219453	-0.55382	-0.48253	-0.28846	Walk	Walk
1.410434	22.59231	1.798447	9.578421	-1.44016	-4.38164	-0.30285	Walk	Walk
1.65744	15.37569	1.052843	6.349337	-5.86132	-7.8176	-4.45269	Walk	Walk
1.089567	14.55721	6.338692	5.278227	-2.17903	-9.46145	-2.56397	Walk	Walk
1.383344	11.29698	14.80006	1.718851	-2.51305	-0.07808	-4.06595	Walk	Walk
1.472854	18.28798	9.901327	5.329856	-3.02162	-5.44776	-2.19251	Walk	Walk
1.92775	11.56843	4.200685	9.736531	-7.77267	-7.32211	-2.04086	Walk	Walk
1.173077	20.76301	18.15975	8.17315	-1.17053	-3.16345	-2.72149	Walk	Walk
1.926193	11.54327	14.61023	3.338215	-5.18399	-5.8118	-0.82084	Walk	Walk
1.819176	14.97792	1.277061	9.831904	-6.49746	-5.43557	-1.00711	Walk	Walk
1.434733	21.77511	2.330646	9.067073	-3.52216	-9.64739	-1.32912	Walk	Walk
1.863143	11.00946	11.52604	1.162329	0	-1.21184	-1.71204	Walk	Walk
1.262655	16.63429	0.532001	0.237267	-5.16088	-8.10479	-3.33733	Walk	Walk
1.110653	9.273631	5.406437	2.018404	-1.06112	-5.70203	-4.33905	Walk	Walk
1.488123	13.77084	3.65867	4.108692	-3.66748	-7.99916	-0.65374	Walk	Walk
1.042231	14.56192	8.545234	6.918341	-3.06876	-0.03845	-0.39219	Walk	Walk
1.143639	24.48401	17.1505	4.288339	-7.93687	-7.29152	-4.55321	Walk	Walk
1.874615	19.46747	16.64779	0.496513	-5.92495	-9.81432	-0.13691	Walk	Walk
1.415744	16.63281	11.93523	1.765934	-7.25023	-0.98412	-3.12336	Walk	Walk
1.604198	5.327823	9.476357	7.160886	-0.1024	-8.26857	-4.55666	Walk	Walk
1.37898	23.37437	9.391372	2.573737	0	-8.97104	-1.82543	Walk	Walk
1.988587	12.28229	6.077591	2.829724	-4.90629	-1.86149	-1.10586	Walk	Walk
1.605094	24.5209	4.198978	4.152925	-1.3654	-3.56192	-2.69434	Walk	Walk
1.735135	12.18187	4.808983	7.431851	0	-1.13807	-3.98688	Walk	Walk
1.936699	11.45713	1.210718	4.034446	-0.34603	-5.00112	-2.20954	Walk	Walk
1.63776	15.95348	8.812045	2.300347	-6.93435	-2.82565	-1.82729	Walk	Walk
1.697395	9.0175	3.221984	2.799533	0	-8.66569	-3.11601	Walk	Walk
1.940895	6.662316	10.14002	6.643793	-5.68527	-7.43097	-0.67331	Walk	Walk
1.547441	10.10408	3.749387	6.958228	0	-5.75797	-0.71126	Walk	Walk
1.057992	24.42645	5.131496	0.108766	-3.91696	-3.21841	-0.7413	Walk	Walk
1.670168	11.85462	12.00736	9.972344	0	-2.50689	-1.5394	Walk	Walk
1.689533	16.14131	18.34273	4.203931	-6.25874	-8.17658	-4.53171	Walk	Walk
1.159364	23.31668	6.862885	9.943069	-3.6803	-9.14195	-4.18942	Walk	Walk
1.574482	8.055679	12.21941	2.678212	-2.01446	-6.85871	-2.7746	Walk	Walk
1.999063	9.375647	13.93673	1.543567	-1.77089	-9.54463	-3.70395	Walk	Walk

Maximum	Pitch_max	Roll_max	Yaw_max	Pitch_min	Roll_min	Yaw_min	F-ADL	Move
1.508293	20.47545	13.19983	1.251049	-5.19996	-6.41822	-1.2625	Walk	Walk
1.650468	8.508581	14.1826	1.976626	0	-4.33266	-4.46815	Walk	Walk
1.706396	9.816728	18.26094	0.992119	-5.39877	-5.32161	-2.02868	Walk	Walk
1.311264	11.19348	5.638559	0.436395	-5.74365	-7.71121	-2.06956	Walk	Walk
4.129863	22.46224	22.1171	13.17323	-11.8702	-1.35181	-1.95253	Run	Run
3.698206	21.45742	23.13311	12.46271	-10.1157	-1.8678	-1.16791	Run	Run
3.223906	18.91625	16.74481	4.836547	-9.80459	-5.76432	-9.32336	Run	Run
3.391089	18.94147	17.66805	4.232976	-3.58686	-6.55967	-7.09638	Run	Run
4.421013	32.9328	27.71967	19.58531	0	-13.2726	-0.02915	Run	Run
2.935171	19.17952	20.52787	9.75185	-5.09061	-2.74912	-1.87236	Run	Run
3.277468	16.95053	24.06837	11.846	-8.10237	-8.20473	-0.66262	Run	Run
3.956272	22.18779	32.09087	10.31315	-1.18809	-3.78697	-9.91082	Run	Run
4.755563	27.71721	34.4507	14.93052	-2.6672	-1.85492	-2.50832	Run	Run
5.443918	21.62044	32.9965	9.077983	-5.39659	-1.06929	-0.23246	Run	Run
5.464401	23.97641	17.8704	9.369314	-7.60912	-11.4631	-3.61996	Run	Run
4.554526	29.6739	32.23494	13.95465	-5.51553	-5.10803	-5.51426	Run	Run
2.595783	28.67026	23.87847	9.15563	-1.76213	-13.3703	-4.88628	Run	Run
4.485562	30.74957	24.89682	10.67146	-7.89486	-1.44082	-7.88512	Run	Run
4.98321	18.96274	20.02535	9.790906	-9.47905	-12.4565	-9.7585	Run	Run
2.60361	20.72205	30.45818	6.916093	-2.01042	-0.626	-1.62949	Run	Run
3.628285	24.60626	21.15987	8.714907	-4.99416	-11.2781	-7.978	Run	Run
2.848935	18.13867	28.67967	14.21909	-9.2309	-2.64877	-1.01351	Run	Run
3.565739	15.44159	19.64794	9.190292	-10.5666	-5.21669	-0.8343	Run	Run
2.71819	34.72373	15.22953	7.020407	-5.51601	-2.96169	-7.19651	Run	Run
3.363765	31.79855	25.47044	13.24677	-7.0298	-4.70562	-2.22302	Run	Run
3.003155	32.54102	21.91807	12.22273	0	-8.7125	-3.10064	Run	Run
3.943887	20.45755	32.81305	10.63484	-5.39386	-3.29226	-6.29464	Run	Run
4.803003	31.63063	34.62714	7.413086	-4.69684	-5.8467	-0.05175	Run	Run
5.299073	27.42232	27.32438	14.33031	-10.2662	-1.85855	-8.73755	Run	Run
2.920613	33.80566	30.75136	8.538959	-0.00119	-1.59979	-8.46027	Run	Run
4.706065	16.28079	33.88153	12.52999	-2.13558	-3.94024	-0.51374	Run	Run
2.885675	32.98028	18.45501	8.724259	-2.58162	-1.38706	-2.05693	Run	Run
4.735406	29.75097	30.97865	8.720806	-1.95704	-14.9175	-0.17854	Run	Run
2.823664	16.6528	31.56339	8.441634	-7.13837	-5.92194	-1.63162	Run	Run
2.593244	31.29548	15.73454	8.584831	0	-0.96632	-7.78633	Run	Run
2.581654	29.3855	19.42078	9.575941	-5.72981	-1.3031	-5.99729	Run	Run

Maximum	Pitch_max	Roll_max	Yaw_max	Pitch_min	Roll_min	Yaw_min	F-ADL	Move
4.672995	26.86956	26.51448	12.65672	-10.4454	-14.4106	-2.87378	Run	Run
5.344393	32.61334	23.37216	14.76212	-8.40425	-1.19223	-2.3657	Run	Run
3.327713	26.25363	22.55019	12.06606	0	-7.90654	-9.9418	Run	Run
3.859197	26.45723	20.63186	12.15963	-1.00513	-5.13016	-3.12234	Run	Run
4.608262	26.48351	21.85581	8.289051	-4.44672	-4.94846	-4.82337	Run	Run
4.025061	22.94916	31.57182	14.71051	-4.30396	-12.4624	-5.79734	Run	Run
3.854532	16.6865	17.38476	14.25008	-5.9287	-3.68815	-9.71251	Run	Run
4.542345	16.48394	27.98314	6.030182	-9.59599	-11.5287	-8.13135	Run	Run
5.408528	26.46326	28.64482	8.476033	-7.31336	-10.1622	-9.62349	Run	Run
2.784208	21.31189	24.6312	9.191159	-4.38547	-10.6838	-9.21081	Run	Run
4.918134	31.5577	17.56559	8.54698	-4.46324	-7.25631	-2.59703	Run	Run
3.257503	28.83037	21.2033	5.341021	-0.69054	-11.325	-1.80935	Run	Run
5.31336	15.57959	31.99987	6.716448	-3.05376	-0.16283	-7.01649	Run	Run
3.318908	28.55738	26.8437	14.73488	-0.62052	-12.135	-8.47008	Run	Run
3.973946	24.91085	24.20742	7.180128	-4.45379	-9.0135	-7.96813	Run	Run
2.700856	29.77147	29.52094	5.922395	-5.87185	-8.85019	-4.37159	Run	Run
5.231374	15.23688	18.39525	9.404931	0	-11.8809	-5.60719	Run	Run
2.85957	18.05133	28.14428	8.662384	-8.49323	-6.7466	-3.02615	Run	Run
4.111181	22.61794	24.21748	12.11548	-1.31199	-12.6179	-0.32058	Run	Run
1.256988	35.33843	14.93188	3.405721	-1.46408	-0.75267	-1.30702	SitDown	SitDown
1.34155	44.91133	13.14171	7.517634	-1.2739	-0.13794	-3.14582	SitDown	SitDown
1.295205	32.27268	11.40939	6.047143	-0.65282	-0.26314	-4.26869	SitDown	SitDown
1.340879	64.87651	21.97016	0.454307	-0.29272	-1.83872	-5.98616	SitDown	SitDown
1.409159	38.75811	3.861453	3.602662	-0.40697	-3.64402	-2.13114	SitDown	SitDown
1.36757	36.68513	15.6403	5.48586	-1.47493	-0.85996	-0.55947	SitDown	SitDown
1.424373	35.07525	9.04174	9.504644	-1.5451	-0.20633	-1.17212	SitDown	SitDown
1.506058	59.78759	19.46872	3.582609	-0.47862	-0.94462	-1.26979	SitDown	SitDown
1.690343	58.63961	7.205038	5.836834	-0.50256	-0.76029	-0.84597	SitDown	SitDown
1.539217	44.92717	8.495678	9.289055	-1.25656	-2.60948	-4.29916	SitDown	SitDown
1.518865	34.40776	16.46848	9.835496	-0.3442	-2.02267	-3.4317	SitDown	SitDown
1.859643	56.77559	6.883199	4.023417	-0.68387	-2.30993	-3.67046	SitDown	SitDown
1.6325	50.46944	8.433635	3.25751	-0.84168	-0.83185	-3.21937	SitDown	SitDown
2.053829	59.06422	14.273	0.488477	-1.18204	-2.26366	-3.26429	SitDown	SitDown
1.542155	33.91949	19.74724	9.292884	-1.3358	-1.17467	-1.25546	SitDown	SitDown
1.585525	40.07197	6.024447	2.555389	-0.39886	-2.43758	-0.23873	SitDown	SitDown
1.326239	34.85776	13.30865	7.960489	-0.82079	-2.76461	-2.21737	SitDown	SitDown

Maximum	Pitch_max	Roll_max	Yaw_max	Pitch_min	Roll_min	Yaw_min	F-ADL	Move
1.229544	41.71435	13.03691	2.421101	-0.94729	-0.00357	-0.8233	SitDown	SitDown
1.110124	48.68482	5.564393	6.027612	-0.97696	-0.99021	-2.99799	SitDown	SitDown
1.681221	56.48387	18.07633	2.974803	-1.14553	-0.87267	-0.35657	SitDown	SitDown
1.582133	38.35729	13.28641	6.398843	-1.13908	-0.61493	-4.95972	SitDown	SitDown
1.751424	55.97578	12.46617	0.479684	-0.45313	-1.50369	-2.70866	SitDown	SitDown
1.65774	39.65101	19.25374	2.33864	-1.42667	-1.62623	-2.54294	SitDown	SitDown
1.377925	58.85947	12.90821	7.751273	-0.02969	-1.79278	-2.68295	SitDown	SitDown
2.04537	45.22355	14.29358	2.463055	-0.50293	-1.22659	-4.95418	SitDown	SitDown
1.87552	38.05937	10.72605	4.870035	-1.09909	-0.62868	-0.77089	SitDown	SitDown
1.696019	53.78842	12.09399	5.455185	-1.41476	-0.26598	-0.40387	SitDown	SitDown
1.354538	56.7692	5.568257	6.462208	-0.03507	-1.89618	-0.43279	SitDown	SitDown
2.060532	48.94642	7.306026	1.022258	-0.95964	-2.1434	-0.64292	SitDown	SitDown
2.012216	56.22907	6.959197	3.677153	-1.22917	-2.34694	-4.73314	SitDown	SitDown
1.289286	40.98683	13.03343	2.236632	-0.00596	-1.37824	-0.5191	SitDown	SitDown
2.045866	32.49111	12.35932	6.773399	-0.32074	-2.9962	-4.43008	SitDown	SitDown
1.830831	31.09345	16.49476	0.104127	-0.90546	-1.14931	-1.64515	SitDown	SitDown
1.111885	41.67307	9.919182	1.357466	-1.19501	-1.87988	-0.15521	SitDown	SitDown
1.444975	52.62992	9.943653	8.547803	-0.67073	-2.62846	-1.4044	SitDown	SitDown
1.905076	53.89142	13.10653	5.341505	-0.78836	-2.24822	-4.98593	SitDown	SitDown
1.127551	40.52077	5.344956	2.408913	-1.11309	-1.07605	-4.01186	SitDown	SitDown
2.049268	31.31947	17.34998	9.001012	-1.06502	-1.57303	-2.95417	SitDown	SitDown
1.97319	42.52449	12.04579	3.051431	-1.21933	-1.21637	-1.65784	SitDown	SitDown
1.998942	49.44515	18.11351	5.747522	-1.17392	-1.35315	-3.5897	SitDown	SitDown
1.948859	30.08756	8.499725	5.489356	-0.9289	-2.72484	-1.80401	SitDown	SitDown
2.059404	50.26177	14.30375	4.67139	-0.78776	-2.76483	-4.48766	SitDown	SitDown
2.057745	57.39653	9.014862	1.049621	-1.25083	-0.61653	-1.78142	SitDown	SitDown
1.103933	31.21751	19.31659	0.448457	-1.35479	-1.49074	-3.67192	SitDown	SitDown
1.525299	31.00149	7.217757	8.001266	-1.34824	-0.12378	-1.44209	SitDown	SitDown
1.233409	43.00283	15.37219	8.933841	-0.87517	-0.79562	-0.10681	SitDown	SitDown
1.255831	58.7578	18.31611	5.337464	-0.48905	-2.49047	-4.04171	SitDown	SitDown
1.926728	54.01183	8.592248	6.601259	-0.90709	-2.13299	-0.46245	SitDown	SitDown
2.05548	34.69231	6.165809	9.660075	-0.88239	-0.66925	-1.8232	SitDown	SitDown
2.064916	52.58716	6.513319	9.160327	-0.68128	-0.19861	-0.15459	SitDown	SitDown
1.205201	18.46211	4.824971	2.032026	-3.41434	-4.17494	-1.85141	StandUp	StandUp
1.467695	13.69013	8.148781	2.019069	-2.79226	-1.78415	-1.58834	StandUp	StandUp
1.484108	43.07633	8.520576	4.756233	-3.97579	-4.17806	-1.21111	StandUp	StandUp

Maximum	Pitch_max	Roll_max	Yaw_max	Pitch_min	Roll_min	Yaw_min	F-ADL	Move
1.506073	15.77872	17.45349	6.52607	-0.1982	-3.76844	-0.56898	StandUp	StandUp
1.664218	21.35648	7.714897	1.090916	-1.91888	-0.34229	-5.20306	StandUp	StandUp
1.511094	21.92414	13.40158	1.187747	-3.27303	-4.30126	-3.77114	StandUp	StandUp
1.200884	21.11708	11.05184	6.037525	-4.16503	-3.72142	-4.59123	StandUp	StandUp
1.567577	22.38214	8.514625	6.234975	-3.78606	-1.24408	-2.17264	StandUp	StandUp
1.6974	24.86003	8.082321	6.648714	-4.50521	-4.9944	-0.56891	StandUp	StandUp
1.366667	21.7693	17.62095	1.775993	-4.63236	-2.04013	-0.17956	StandUp	StandUp
1.451517	28.43403	10.60821	0.064943	-2.28807	-3.91387	-3.15886	StandUp	StandUp
1.175028	27.79274	10.53797	6.710841	-3.97118	-1.33966	-0.74217	StandUp	StandUp
1.405783	31.83283	10.17402	2.367563	-0.92971	-3.77375	-4.71025	StandUp	StandUp
1.473677	16.8848	14.35873	0.866674	-2.65294	-0.119	-3.87587	StandUp	StandUp
1.158298	27.12196	15.27261	4.848938	-0.87044	-1.02659	-0.06671	StandUp	StandUp
1.547754	33.63568	8.066847	1.139607	-2.22643	-1.79173	-2.93941	StandUp	StandUp
1.674846	33.19926	13.98381	1.145862	-2.75048	-3.22944	-3.42363	StandUp	StandUp
1.165942	22.20218	10.45401	0.625019	-1.2623	-3.59724	-4.12506	StandUp	StandUp
1.257421	23.19679	16.75754	5.938772	-2.17891	-1.01102	-1.0191	StandUp	StandUp
1.245659	19.12558	17.55261	0.717587	-1.86614	-2.98343	-0.01439	StandUp	StandUp
1.274137	25.75456	7.650854	5.391563	-2.37667	-3.53947	-1.70892	StandUp	StandUp
1.149258	16.77132	12.44063	1.206473	-1.61118	-1.88503	-0.40883	StandUp	StandUp
1.056093	33.03199	17.23497	5.104676	-3.38408	-1.01039	-2.78067	StandUp	StandUp
1.530102	30.2544	7.922105	0.217563	-3.44316	-4.38665	-1.47736	StandUp	StandUp
1.041063	29.44872	5.50855	5.136365	-3.35462	-2.37559	-4.31088	StandUp	StandUp
1.538546	30.34096	19.66187	4.326017	-2.20019	-0.25508	-1.52098	StandUp	StandUp
1.441583	32.68306	9.050708	1.798324	-4.71372	-4.83115	-1.01341	StandUp	StandUp
1.118984	16.94474	17.04724	5.354529	-1.84783	-3.18953	-1.41373	StandUp	StandUp
1.290985	25.32432	14.0371	1.665536	-2.19412	-1.5788	-0.27272	StandUp	StandUp
1.014996	20.22653	14.40462	4.224755	-2.44301	-4.10907	-3.63169	StandUp	StandUp
1.19315	32.5779	16.70011	3.702048	-0.16177	-4.44421	-3.71155	StandUp	StandUp
1.202279	26.30487	8.808876	3.680148	-1.07475	-3.7129	-0.05306	StandUp	StandUp
1.655173	17.48557	8.58546	5.371711	-0.28299	-4.445	-2.7472	StandUp	StandUp
1.543966	25.04812	15.09897	4.582092	-1.5622	-1.93054	-3.18111	StandUp	StandUp
1.365772	30.16353	12.54612	2.915058	-1.49465	-4.67615	-2.49845	StandUp	StandUp
1.225878	26.43663	12.21587	2.115828	-2.35359	-2.10251	-1.16502	StandUp	StandUp
1.364471	20.42166	17.41597	0.096546	-0.81701	-4.58471	-4.44003	StandUp	StandUp
1.019336	17.21975	12.77878	1.580112	-1.3755	-2.79629	-4.94913	StandUp	StandUp
1.482597	21.62495	12.02364	1.051008	-0.36765	-4.523	-4.65145	StandUp	StandUp

Maximum	Pitch_max	Roll_max	Yaw_max	Pitch_min	Roll_min	Yaw_min	F-ADL	Move
1.476118	19.73966	9.73928	3.457155	-0.56666	-4.90397	-4.90501	StandUp	StandUp
1.657425	18.9088	15.99773	1.398657	-1.13679	-1.11333	-3.85147	StandUp	StandUp
1.163292	30.83406	10.88688	1.994777	-0.12521	-3.51284	-4.23422	StandUp	StandUp
1.03175	19.21257	6.442666	2.298256	-4.58843	-0.90796	-2.7012	StandUp	StandUp
1.22309	20.3196	13.66303	1.295273	-4.49511	-3.94449	-1.08631	StandUp	StandUp
1.640112	19.73113	15.69602	3.015587	-0.64479	-1.54155	-4.86132	StandUp	StandUp
1.355757	19.18763	15.77643	5.092354	-0.66537	-1.89267	-3.41699	StandUp	StandUp
1.334814	17.46038	10.04083	4.803319	-0.594	-0.66921	-3.5507	StandUp	StandUp
1.084335	32.74706	7.812793	1.444612	-4.82884	-3.87888	-0.62351	StandUp	StandUp
1.574234	27.93993	16.90125	6.193485	-4.07578	-2.30177	-0.74749	StandUp	StandUp
8.276207	94.4767	12.39705	6.787408	-4.14199	-2.42781	-0.54718	Fall	FallFor
5.722978	84.78555	13.24851	0.260283	0	0	-3.84542	Fall	FallFor
7.562392	95.6332	8.181265	0.385697	0	-8.96605	-10.9867	Fall	FallFor
6.297566	98.05477	4.393119	3.072094	-0.196	-4.76557	-2.13627	Fall	FallFor
7.573843	80.74953	16.77859	0.302307	-0.21858	-0.00184	-8.28143	Fall	FallFor
7.481774	82.40811	7.015469	0.539995	-3.21247	-8.38392	-3.98144	Fall	FallFor
4.824183	71.52458	11.47641	1.913306	-1.10502	-5.84397	-5.85716	Fall	FallFor
6.159443	102.8999	13.61605	3.740563	-4.95997	-4.75383	-0.8124	Fall	FallFor
4.608132	97.16945	17.97352	0.131602	-1.87399	-4.98581	-9.34251	Fall	FallFor
7.167699	109.9339	12.89782	5.144835	-3.70453	-1.39901	-7.99978	Fall	FallFor
4.556864	80.95132	9.46777	6.421374	-1.80038	-0.56167	-6.82368	Fall	FallFor
5.736863	88.31426	13.36226	0.964011	-3.13154	-9.79325	-8.37328	Fall	FallFor
4.141639	99.80548	10.43516	2.667163	-0.38803	-6.79154	-0.38457	Fall	FallFor
6.063309	76.08532	5.247951	3.924561	-0.21013	-3.95098	-8.3993	Fall	FallFor
8.182396	82.35755	13.44824	6.654239	-2.93652	-3.63872	-8.50539	Fall	FallFor
6.76292	84.35209	6.98769	9.561777	-1.89311	-1.32357	-7.67149	Fall	FallFor
3.936341	79.05331	6.376779	2.659849	-2.7405	-3.74247	-3.75819	Fall	FallFor
4.669075	101.1175	19.78604	7.90778	-2.19755	-0.82409	-0.47547	Fall	FallFor
4.045396	74.42581	17.49625	8.919099	-3.56903	-0.90865	-4.77114	Fall	FallFor
5.138752	109.0325	12.18807	5.435534	-4.1021	-0.61813	-6.83881	Fall	FallFor
7.57373	105.4725	18.63656	8.802352	-1.7181	-4.15537	-9.31319	Fall	FallFor
8.095484	90.59067	13.58028	0.91003	-4.44968	-5.41195	-0.09208	Fall	FallFor
6.614596	95.65226	8.62666	6.496105	-2.75475	-5.83719	-7.32166	Fall	FallFor
4.740026	105.1973	5.250578	8.421176	-3.837	-3.49416	-5.12839	Fall	FallFor
8.041403	96.46273	5.874866	4.153769	-1.5087	-1.42374	-8.71139	Fall	FallFor
4.711715	46.48073	6.114928	20.99355	-93.446	-10.689	-0.88589	Fall	FallBac

Maximum	Pitch_max	Roll_max	Yaw_max	Pitch_min	Roll_min	Yaw_min	F-ADL	Move
3.587695	44.80042	4.406589	3.698869	-92.725	-8.30875	-5.69065	Fall	FallBac
6.387436	38.12261	15.10777	4.083906	-71.7017	0	-5.73079	Fall	FallBac
3.972074	52.5523	0.540514	10.59791	-83.3364	-11.2246	-2.22441	Fall	FallBac
7.954954	32.15308	17.15907	23.42527	-87.1639	0	-0.89161	Fall	FallBac
4.801371	43.74305	4.223157	13.12026	-86.617	-6.96272	-0.78017	Fall	FallBac
8.37398	35.92743	2.46145	2.748124	-79.5528	-6.96823	-3.35052	Fall	FallBac
9.091715	32.93173	2.029946	11.55232	-77.6239	-24.3228	0	Fall	FallBac
9.415081	47.56971	15.09434	15.4494	-105.582	-18.5354	-2.65069	Fall	FallBac
8.018073	38.69885	16.21099	13.98239	-84.5209	-9.19261	-4.73304	Fall	FallBac
7.762866	49.12387	10.72038	5.362746	-99.8762	-17.7472	-3.19696	Fall	FallBac
8.653055	38.31791	18.60117	10.79477	-71.9099	-3.79337	-4.99537	Fall	FallBac
9.387481	31.33409	11.67523	17.94143	-77.5344	-0.82835	-1.18956	Fall	FallBac
4.947574	33.06907	19.84666	9.619332	-85.0128	-14.8504	-0.66419	Fall	FallBac
3.843035	44.4938	5.654161	7.112774	-79.7589	-11.0297	-0.16043	Fall	FallBac
3.703097	42.15662	8.32237	9.927584	-82.5606	-1.45528	-4.6281	Fall	FallBac
5.136902	47.43513	6.993219	5.391958	-78.5535	-11.1355	-1.15433	Fall	FallBac
4.631158	49.73551	0.050196	7.271072	-95.4129	-7.8563	-2.74871	Fall	FallBac
8.538274	45.32092	6.359704	19.54121	-108.775	-5.11683	-3.88108	Fall	FallBac
7.602613	48.88015	4.228232	3.534834	-72.1782	-15.9496	-3.32362	Fall	FallBac
5.421073	33.49419	13.69796	9.301285	-106.5	-13.1041	-1.27592	Fall	FallBac
4.807484	39.92139	17.88397	12.64163	-105.973	-17.0159	-4.9109	Fall	FallBac
6.122518	47.61899	6.516218	2.342738	-93.8587	-19.6953	-2.1279	Fall	FallBac
7.919397	41.27495	8.684043	9.618513	-97.9775	-11.4678	-0.53312	Fall	FallBac
7.067423	30.45687	8.987747	2.415064	-77.5245	-1.23278	-2.61539	Fall	FallBac
3.174922	42.73672	51.414	124.7973	-17.2791	-0.55126	-2.87799	Fall	FallRight
3.99048	36.36859	42.49311	104.6308	-23.2814	-0.38915	-1.67644	Fall	FallRight
8.103662	44.38821	30.26959	84.69834	-0.76381	-9.25921	-0.13219	Fall	FallRight
6.228679	36.25064	16.27974	110.5346	0	-5.30039	-2.35826	Fall	FallRight
5.994513	24.4116	24.27248	121.1515	-26.1999	-4.54916	-1.9619	Fall	FallRight
5.750129	38.59155	53.08385	109.0003	0	-0.03491	-2.54887	Fall	FallRight
5.307713	30.68719	79.35879	106.843	-24.8981	-0.02528	-0.43517	Fall	FallRight
6.770977	19.45486	103.275	97.23511	-15.0084	-0.4928	-0.5222	Fall	FallRight
4.475686	27.47764	92.40968	110.1403	-5.82042	-0.01481	-0.29472	Fall	FallRight
8.007923	30.93208	46.66113	124.9848	-16.0429	-5.75011	-2.64157	Fall	FallRight
4.314217	26.49218	39.5149	121.6729	-10.8542	-5.92172	-2.42675	Fall	FallRight
6.079298	31.82116	96.08056	85.67212	-6.10402	-2.75213	-2.26048	Fall	FallRight

Maximum	Pitch_max	Roll_max	Yaw_max	Pitch_min	Roll_min	Yaw_min	F-ADL	Move
8.011147	40.41131	82.79818	122.8541	-19.4308	-5.51513	-2.64833	Fall	FallRight
4.768217	30.45252	106.329	112.0696	-22.1961	-1.35265	-1.22142	Fall	FallRight
3.851239	24.32225	85.28916	125.481	-20.0307	-9.92011	-1.68955	Fall	FallRight
7.996487	26.12038	33.82128	83.93191	-0.30467	-9.89815	-1.35992	Fall	FallRight
3.518249	35.94095	81.86101	121.0729	-15.8872	-0.06436	-1.74648	Fall	FallRight
7.332211	31.84976	49.12126	121.1106	-0.89808	-9.46332	-2.37525	Fall	FallRight
5.366805	23.58306	105.9877	127.02	-13.4947	-6.52181	-2.48386	Fall	FallRight
8.412377	33.96744	72.95007	97.1188	-5.56859	-7.33909	-0.80158	Fall	FallRight
7.177483	44.6241	87.98275	126.8772	-16.1723	-5.50374	-1.01617	Fall	FallRight
8.979591	29.62065	44.81245	83.22498	-19.2429	-8.82083	-1.10041	Fall	FallRight
5.118609	43.28162	54.84102	116.0579	-15.5391	-2.23659	-0.51681	Fall	FallRight
7.544948	38.73186	34.46463	86.12964	-12.5644	-2.83826	-2.93779	Fall	FallRight
6.699691	36.50248	108.1099	110.9036	-10.7449	-9.03664	-2.3852	Fall	FallRight
4.206187	32.25469	14.08069	4.028107	-6.9391	-44.0174	-114.911	Fall	FallLeft
4.675028	36.29375	0.157854	4.253528	0	-63.9515	-122.628	Fall	FallLeft
6.499905	26.14337	1.513272	1.01201	-29.936	-74.2203	-70.6173	Fall	FallLeft
5.643128	30.86171	2.02826	4.153311	-16.48	-68.1033	-66.1634	Fall	FallLeft
4.119604	37.52556	6.316024	0.364995	-24.289	-22.0643	-74.2529	Fall	FallLeft
8.810262	39.91611	3.118249	2.749729	-6.22963	-67.7531	-128.745	Fall	FallLeft
7.119994	33.02155	7.996029	1.130901	-6.31116	-73.4471	-84.3127	Fall	FallLeft
7.081222	37.86091	0.482991	2.955773	-24.9095	-30.9044	-94.0528	Fall	FallLeft
5.244338	37.03225	14.85333	3.984965	-15.4058	-50.0728	-74.5242	Fall	FallLeft
3.954763	43.43271	4.586636	0.784886	-0.38397	-49.351	-112.456	Fall	FallLeft
3.540011	34.52037	0.756934	0.24833	-7.15975	-73.5252	-127.71	Fall	FallLeft
7.014268	30.51368	9.188681	3.827348	-0.35503	-68.4737	-70.2915	Fall	FallLeft
5.336154	40.35031	11.47735	0.367485	-21.2244	-59.8634	-96.9999	Fall	FallLeft
6.817239	31.89571	12.91131	4.2829	-4.56609	-34.9141	-118.999	Fall	FallLeft
6.142545	28.41579	7.475992	0.018283	-9.42068	-70.5765	-120.624	Fall	FallLeft
8.635523	27.86669	9.016951	2.338658	-4.75005	-37.1813	-103.062	Fall	FallLeft
8.490714	42.67006	11.9692	1.213549	-21.7635	-43.6649	-82.2592	Fall	FallLeft
6.162296	33.16095	14.48292	4.68237	-13.4847	-38.3594	-106.789	Fall	FallLeft
8.367948	29.82961	5.205827	3.470085	-6.94076	-74.8965	-82.1921	Fall	FallLeft
7.919353	36.50306	1.846743	4.846173	-11.7808	-50.6285	-111.04	Fall	FallLeft
8.568915	27.42463	11.96038	1.130113	-1.42327	-65.6178	-100.169	Fall	FallLeft
6.854588	39.84193	13.88021	4.475582	-15.8679	-29.8505	-123.638	Fall	FallLeft
9.207054	32.92744	4.126116	0.900329	-1.73805	-31.3906	-101.399	Fall	FallLeft

Maximum	Pitch_max	Roll_max	Yaw_max	Pitch_min	Roll_min	Yaw_min	F-ADL	Move
5.79078	26.53459	5.802834	3.958147	-18.4327	-65.7068	-114.748	Fall	FallLeft
8.473119	38.56479	2.036331	2.786568	-0.17652	-45.6327	-118.449	Fall	FallLeft
7.176917	6.19923	8.482907	2.500762	-49.8177	-57.5673	-59.6081	Fall	FallBTR
3.94341	24.16548	0.01731	3.740255	-59.1546	-58.4408	-60.606	Fall	FallBTR
4.119604	37.52556	6.316024	4.957875	-48.1738	-22.0643	-58.7327	Fall	FallBTR
5.54466	28.2688	3.564812	9.480833	-42.9673	-34.2311	-44.362	Fall	FallBTR
8.302212	11.42061	3.372094	1.853723	-45.1438	-31.9605	-50.3038	Fall	FallBTR
7.012113	41.38842	9.783025	3.739333	-47.3089	-55.5963	-56.1667	Fall	FallBTR
6.25032	9.485554	1.661768	9.453437	-54.4147	-46.9073	-51.9517	Fall	FallBTR
7.974633	35.78964	2.02732	2.319958	-51.3873	-22.0771	-62.6042	Fall	FallBTR
4.585585	42.02268	3.288512	3.901341	-55.7246	-33.3275	-51.7686	Fall	FallBTR
4.542851	21.70321	8.96785	4.753557	-49.2573	-43.4993	-45.0468	Fall	FallBTR
3.710443	31.64434	9.817571	4.52513	-40.1253	-28.4386	-53.6614	Fall	FallBTR
5.098959	15.74374	4.40892	9.482449	-55.4891	-57.5211	-63.1153	Fall	FallBTR
7.261697	29.09508	5.032414	1.926933	-56.0163	-24.4058	-45.4581	Fall	FallBTR
9.288839	13.70466	0.607418	1.935383	-58.7135	-40.1085	-47.3164	Fall	FallBTR
8.392615	29.72431	8.494257	3.148619	-44.0472	-52.8658	-48.1566	Fall	FallBTR
5.823923	12.16866	8.411568	2.028616	-49.5245	-46.6349	-52.4586	Fall	FallBTR
7.242063	30.30717	3.56726	6.272428	-44.425	-25.6685	-42.1429	Fall	FallBTR
3.516758	22.78722	3.326	9.190139	-53.2609	-56.5635	-54.575	Fall	FallBTR
4.276657	17.68926	6.189744	4.868554	-47.2072	-29.9529	-52.0891	Fall	FallBTR
4.798956	25.70638	1.657342	7.620798	-49.115	-20.8898	-41.9248	Fall	FallBTR
5.536104	23.59587	8.753393	5.330736	-53.9673	-30.2522	-45.7578	Fall	FallBTR
4.387509	31.69232	9.333112	4.082398	-46.9565	-35.6438	-60.0201	Fall	FallBTR
5.070857	9.087767	8.470675	2.666568	-43.2479	-22.8596	-50.5994	Fall	FallBTR
7.258258	12.26102	2.462276	4.286949	-55.9747	-30.01	-57.5649	Fall	FallBTR
6.011493	39.09608	5.704433	3.257975	-44.4584	-55.5896	-61.901	Fall	FallBTR
3.552171	36.36093	68.83903	49.30513	-75.938	-3.8126	-2.98115	Fall	FallBTL
5.615542	27.31431	5.935033	61.17977	-60.976	-14.945	-1.029	Fall	FallBTL
5.454638	26.95846	25.07416	56.6101	-73.3413	-21.0109	-3.10626	Fall	FallBTL
5.463831	28.24578	51.39127	50.71659	-64.6597	-4.62551	-0.04718	Fall	FallBTL
5.66995	33.96556	28.83084	69.66618	-58.0825	-11.198	-1.29108	Fall	FallBTL
5.195287	32.9974	27.06963	41.53208	-60.2481	-14.4136	-3.63513	Fall	FallBTL
6.801044	27.467	63.81972	43.93852	-56.0964	-10.8311	-2.92811	Fall	FallBTL
7.028998	27.48677	59.60225	43.91181	-74.6876	-5.22811	-4.09192	Fall	FallBTL
7.096964	28.92425	69.83876	61.82816	-61.6749	-0.45916	-1.67035	Fall	FallBTL

Maximum	Pitch_max	Roll_max	Yaw_max	Pitch_min	Roll_min	Yaw_min	F-ADL	Move
8.976769	26.37554	49.90158	52.63287	-70.2753	-1.01841	-2.42316	Fall	FallBTL
4.8809	29.34146	58.80941	53.50277	-64.7313	-11.924	-0.17769	Fall	FallBTL
4.176955	34.82781	33.76984	64.45947	-71.8952	-19.0136	-4.89107	Fall	FallBTL
4.445665	26.26033	60.18924	42.02139	-71.5883	-6.44398	-4.77507	Fall	FallBTL
6.359866	28.62425	57.73388	50.72174	-73.6315	-16.306	-3.11237	Fall	FallBTL
6.833618	36.37339	58.12073	62.44278	-71.8262	-6.5094	-0.03298	Fall	FallBTL
5.288334	35.83032	39.37522	40.40823	-72.7119	-7.29219	-2.34684	Fall	FallBTL
7.573779	31.47452	52.58259	56.9361	-74.5126	-10.8686	-1.37733	Fall	FallBTL
6.824611	34.76433	42.62602	58.04873	-71.4292	-19.1533	-4.6018	Fall	FallBTL
7.128076	34.87445	50.63282	51.67918	-73.7103	-11.2333	-2.88558	Fall	FallBTL
4.301884	39.47182	44.27219	46.52132	-68.7897	-10.1833	-4.72306	Fall	FallBTL
9.399623	33.59505	34.53912	62.51216	-61.4647	-11.4909	-0.16849	Fall	FallBTL
4.452988	25.54713	67.48015	56.23614	-73.2936	-17.2048	-1.19076	Fall	FallBTL
9.465304	39.10383	50.51205	48.23371	-65.2123	-3.62921	-1.66439	Fall	FallBTL
9.339755	36.501	58.92422	58.89399	-69.8432	-0.75752	-4.03732	Fall	FallBTL
5.869405	26.98009	63.8559	69.10266	-56.6947	-8.66636	-0.38516	Fall	FallBTL

東海大學
資訊工程學系

TUNGHAI UNIVERSITY COMPUTER SCIENCE DEPARTMENT
1981
東海大學
資訊工程學系